ELECTRONIC SUPPLEMENTARY INFORMATION

Synthesis, structural studies and stability of the model, cysteine containing DNA-protein cross-links

Kinga Salus, Marcin Hoffmann, Tomasz Siodła, Bożena Wyrzykiewicz,
Donata Pluskota-Karwatka*

Adam Mickiewicz University in Poznań, Faculty of Chemistry, Umultowska 89b,
61-614 Poznań, Poland
e-mail: donatap@amu.edu.pl

Chromatograms of reaction mixtures and of solutions subjected to stability studies

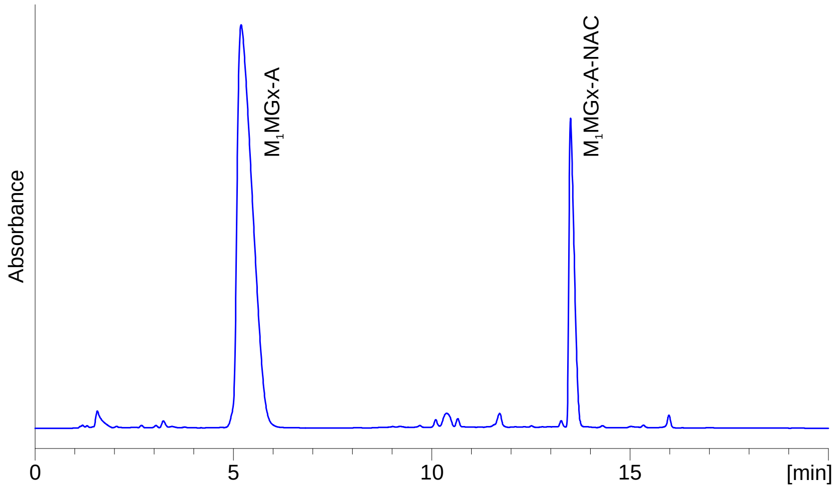

Fig. S1. C18 analytical column LC-DAD chromatogram (recorded at 254 nm) of the reaction mixture of M_1MGx-A with NAC in 0.1 M PB held at 37 °C for 24 h.

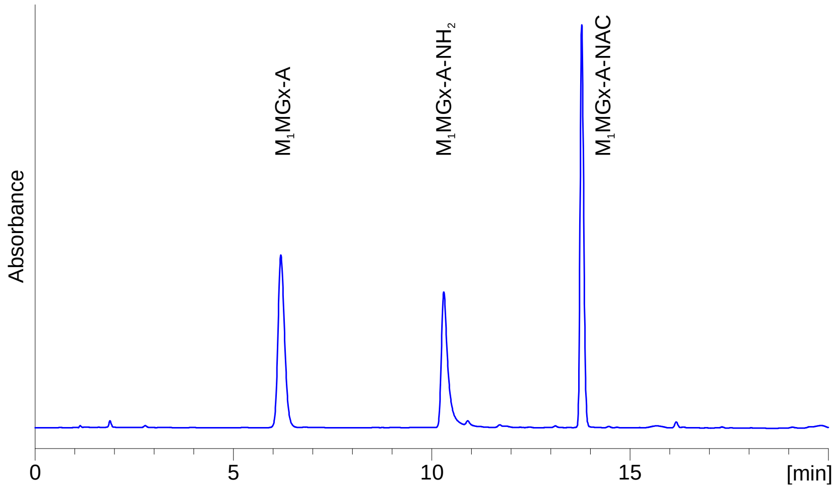

Fig. S2. C18 analytical column LC-DAD chromatogram (recorded at 254 nm) of the M_1MGx-A-NAC solution in 0.1 M PB held at 37 °C for 9 days.

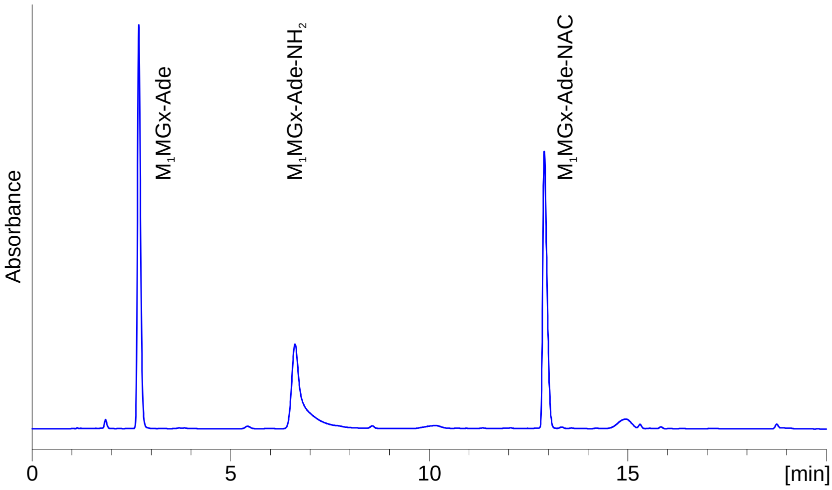

Fig. S3. C18 analytical column LC-DAD chromatogram (recorded at 254 nm) of the M_1MGx-Ade-NAC solution in 0.1 M PB held at 37 °C for 12 days.

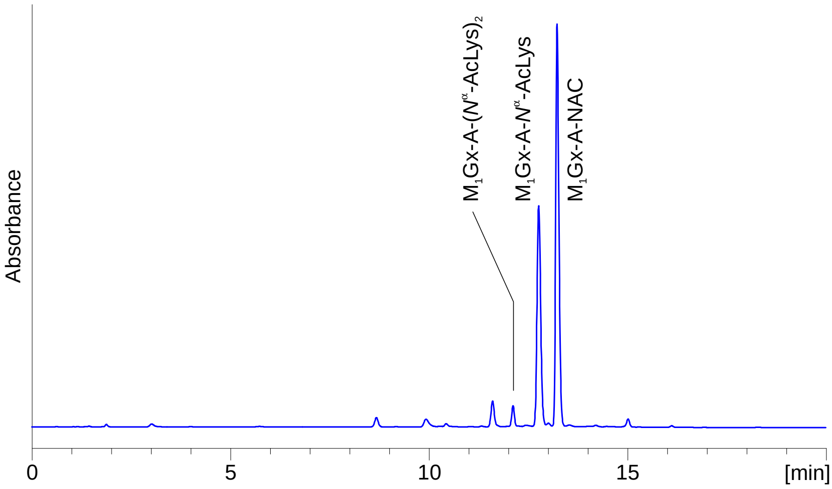

Fig. S4. C18 analytical column LC-DAD chromatogram (recorded at 254 nm) of the M_1Gx-A-NAC mixture with N^{α}-acetyllysine in 0.1 M PB solution held at 37 °C for 15 min.

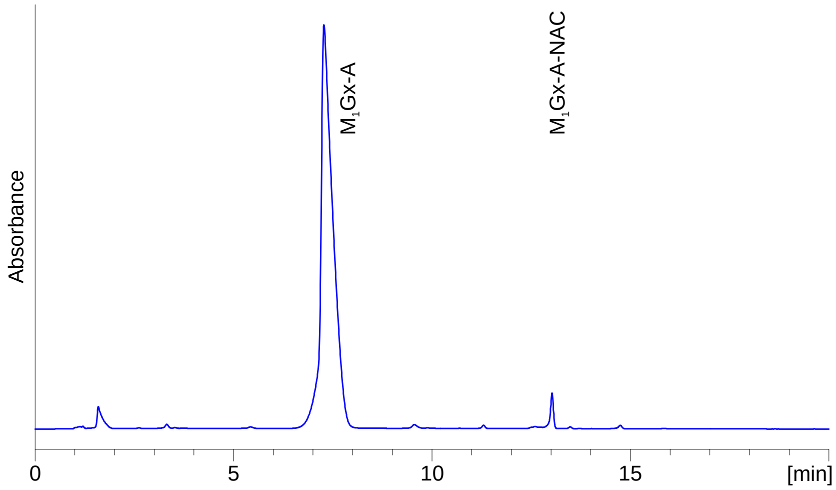

Fig. S5. C18 analytical column LC-DAD chromatogram (recorded at 254 nm) of the reaction mixture of M$_1$Gx-A with NAC and *N*$^{\alpha}$-acetyllysine in 0.1 M PB held at 37 °C for 3 h.

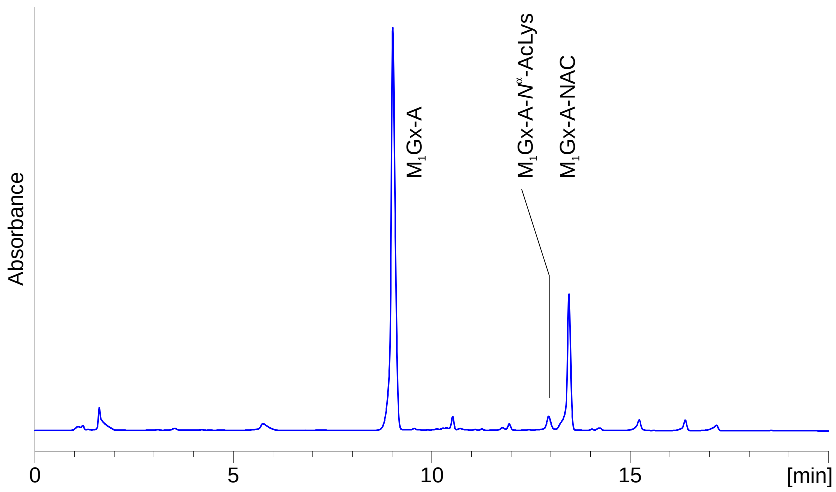

Fig. S6. C18 analytical column LC-DAD chromatogram (recorded at 254 nm) of the reaction mixture of M$_1$Gx-A with NAC and *N*$^{\alpha}$AcLys in 0.1 M PB held at 37 °C for 26 h.

NMR data of M_1MGx-Ade-NAC

Table S1. NMR data of M_1MGx-Ade-NAC (D_2O, standard NMR – TSP-d_4)

	δ(H) [ppm]	Multiplicity	$J_{H.H}$ [Hz]	δ(C) [ppm]	HMBC
CHO	9.56	s		194.13	C7, C8, C1”, C2”
C1”				127.50	
C2”	8.72			171.44	C7, CHO, Cβ
CH_3	2.31	s (split)		15.07	C7, C8, C1”, C2”, CHO
H-C2	8.29	s		143.45	C3a, C9a, C9b
C3a				141.98	
H-C5	8.52	s (split)		138.11	C3a, C7, C9a
C7				115.41	
C8				145.27	
C9a				146.07	
C9b				118.43	
CH_3 (Ac)	2.05	s (split)		24.88	C=O (Ac)
C=O (Ac)				176.54	
H-Cα	4.56	td	4.25; 8.02	57.74	Cβ, C=O (Ac)
Ha-Cβ	3.39	dd (split)	8.36; 14.24	40.49	Cα, C2”, COOH
Hb-Cβ	3.64	dd (split)	4.30; 13.79		Cα, C2”, COOH
COOH				178.31	

Mass spectra of studied compounds

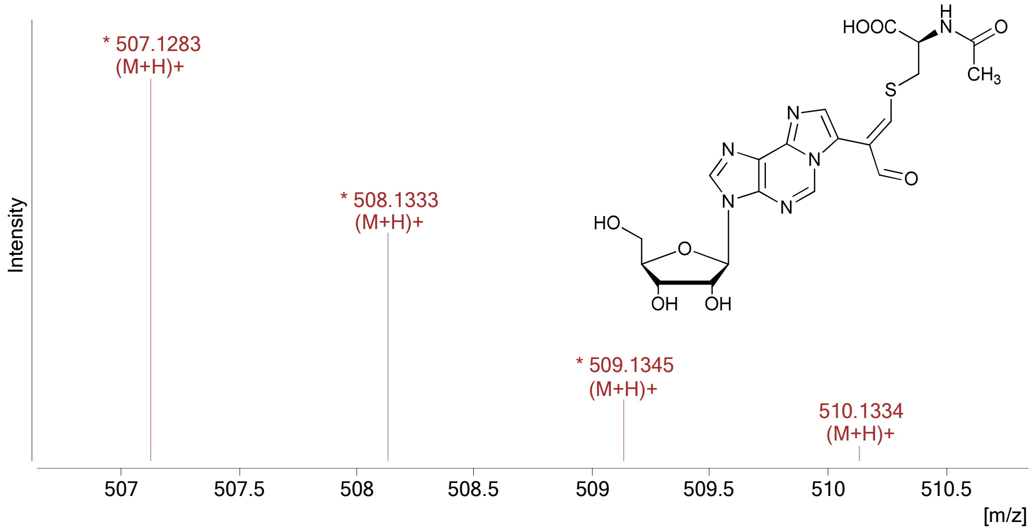

Fig. S7. Positive ions MS spectrum of M_1Gx-A-NAC

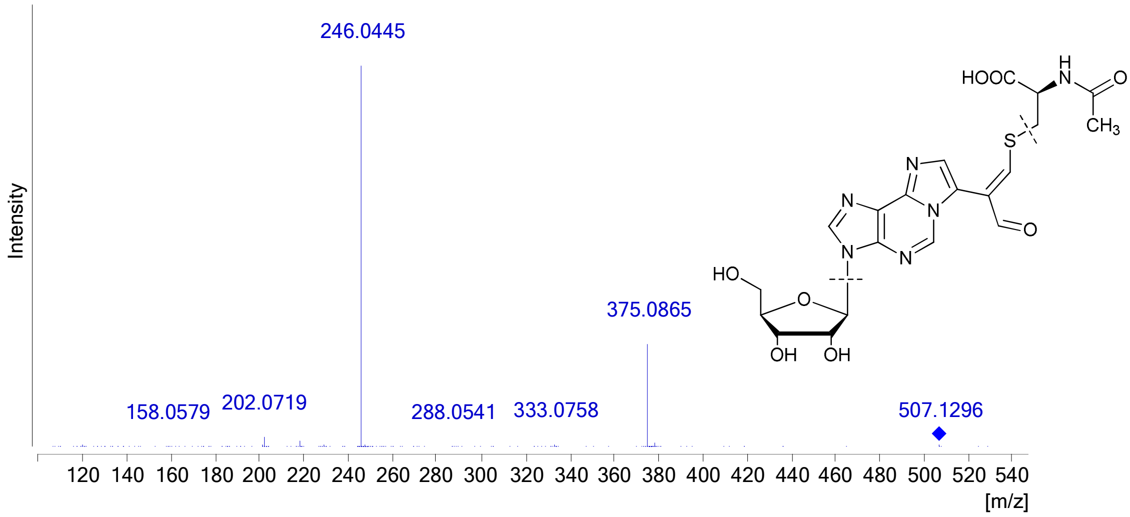

Fig. S8. Positive ions MS/MS spectrum of M_1Gx-A-NAC; collision energy 30 eV

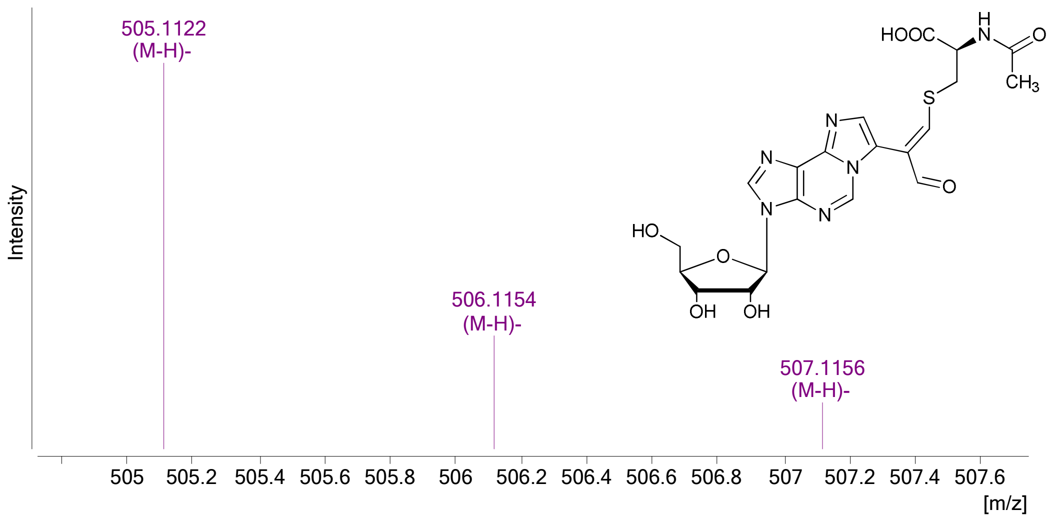

Fig. S9. Negative ions MS spectrum of M_1Gx-A-NAC

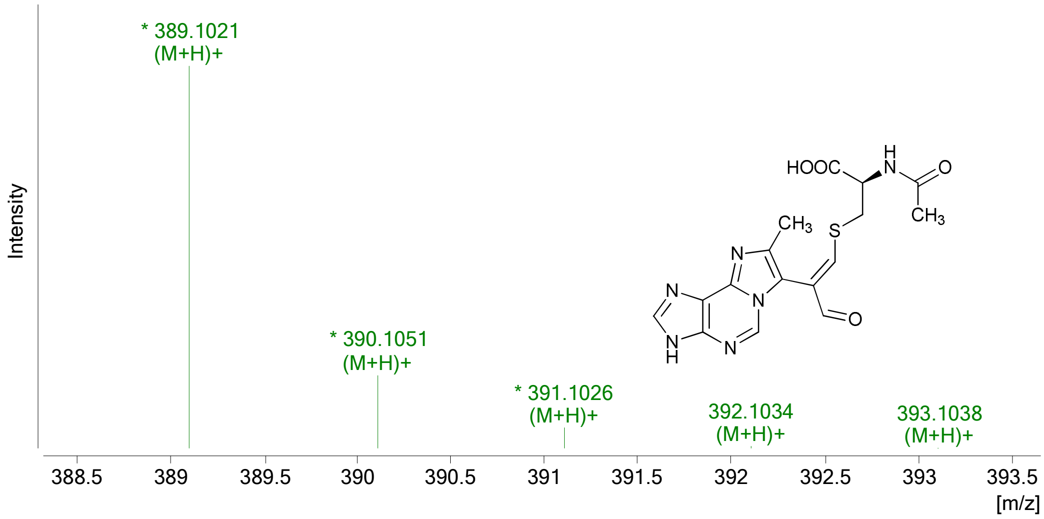

Fig. S10. Positive ions MS spectrum of M_1MGx-Ade-NAC

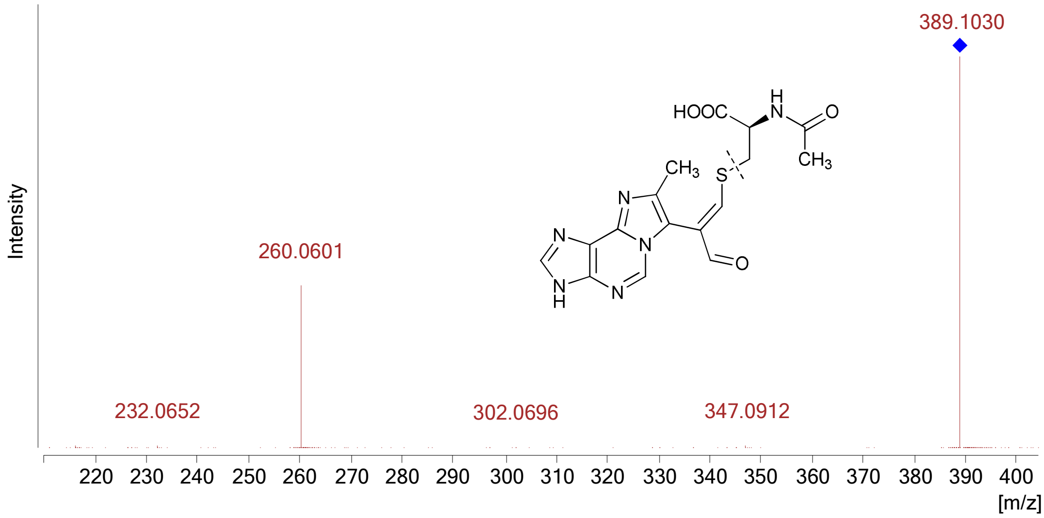

Fig. S11. Positive ions MS/MS spectrum of M_1MGx-Ade-NAC; collision energy 10 eV

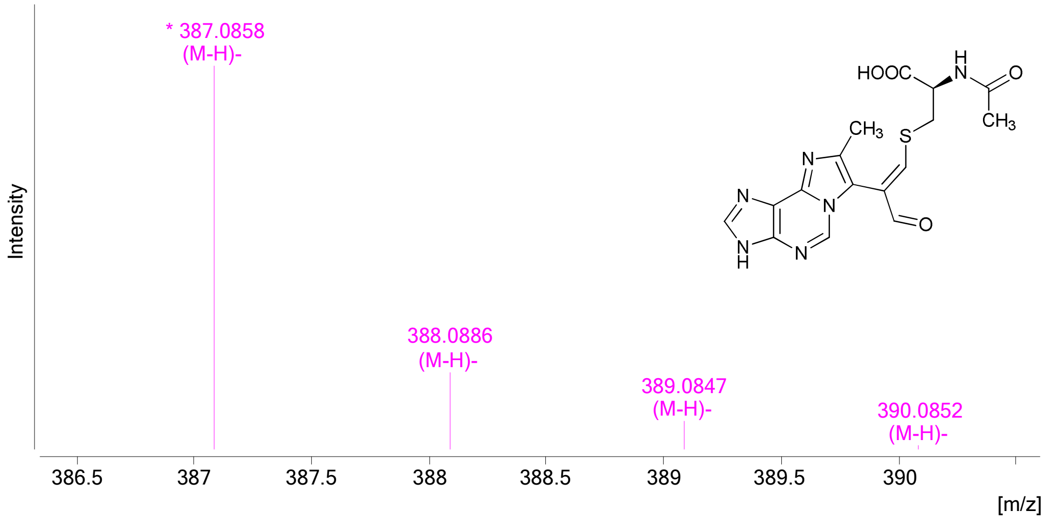

Fig. S12. Negative ions MS spectrum of M_1MGx-Ade-NAC

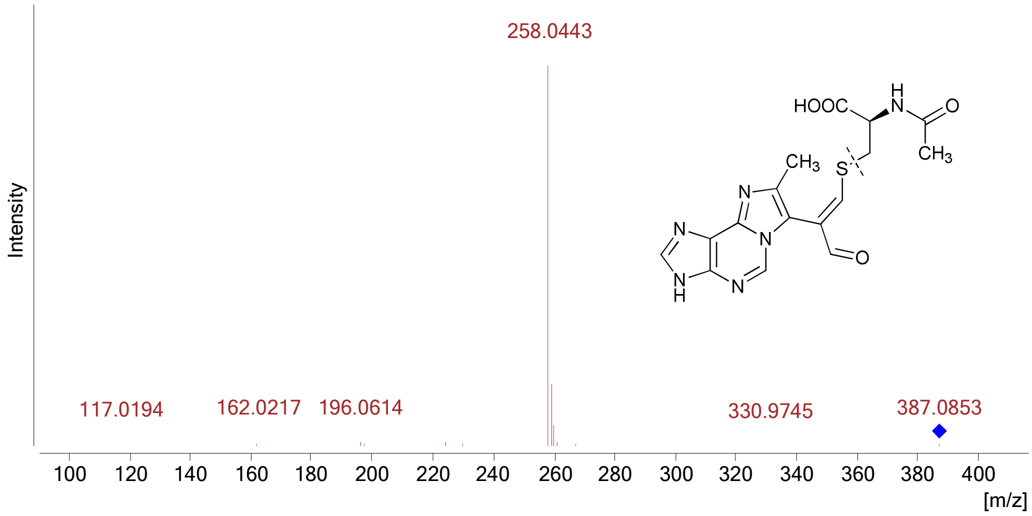

Fig. S13. Negative ions MS/MS spectrum of M_1MGx-Ade-NAC; collision energy 10 eV

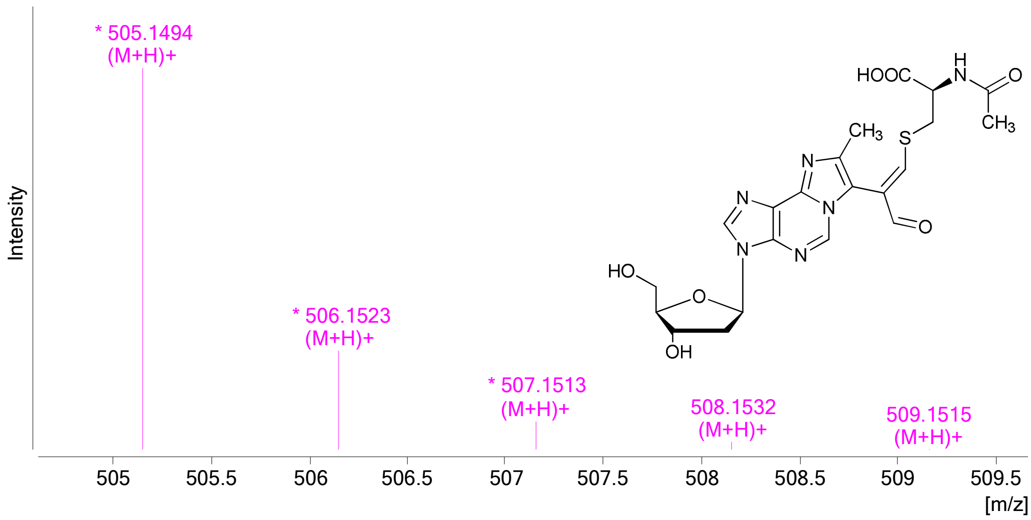

Fig. S14. Positive ions MS spectrum of M_1MGx-dA-NAC

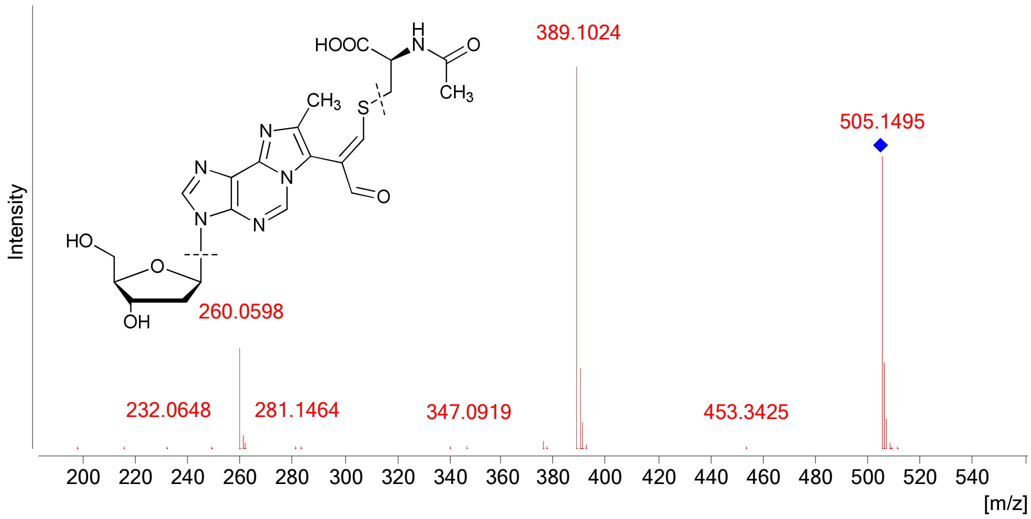

Fig. S15. Positive ions MS/MS spectrum of M_1MGx-dA-NAC; collision energy 15 eV

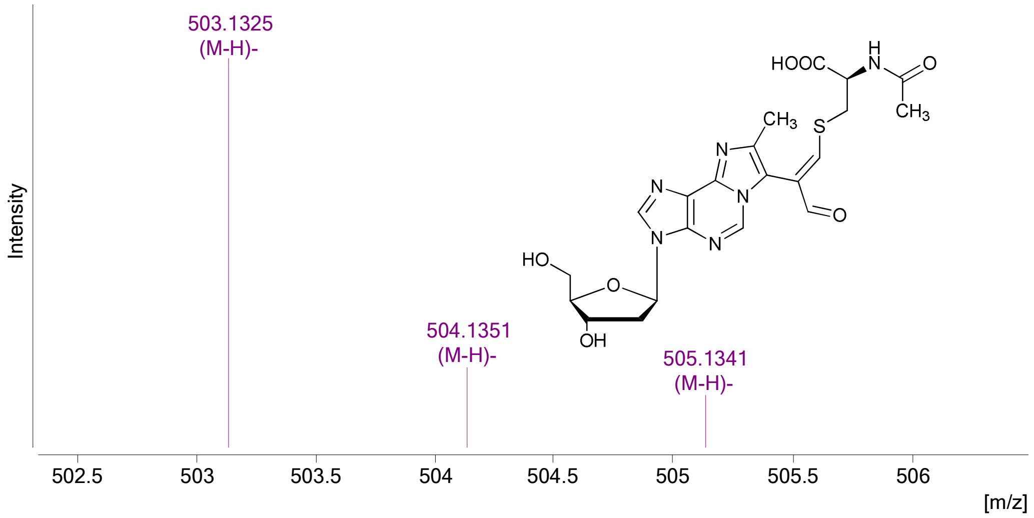

Fig. S16. Negative ions MS spectrum of M_1MGx-dA-NAC

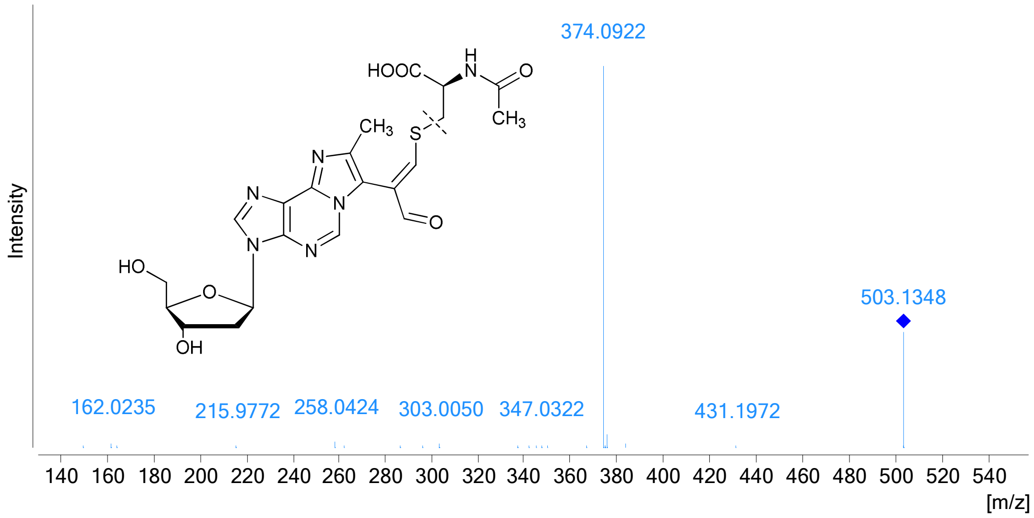

Fig. S17. Negative ions MS spectrum of M_1MGx-dA-NAC; collision energy 10 eV

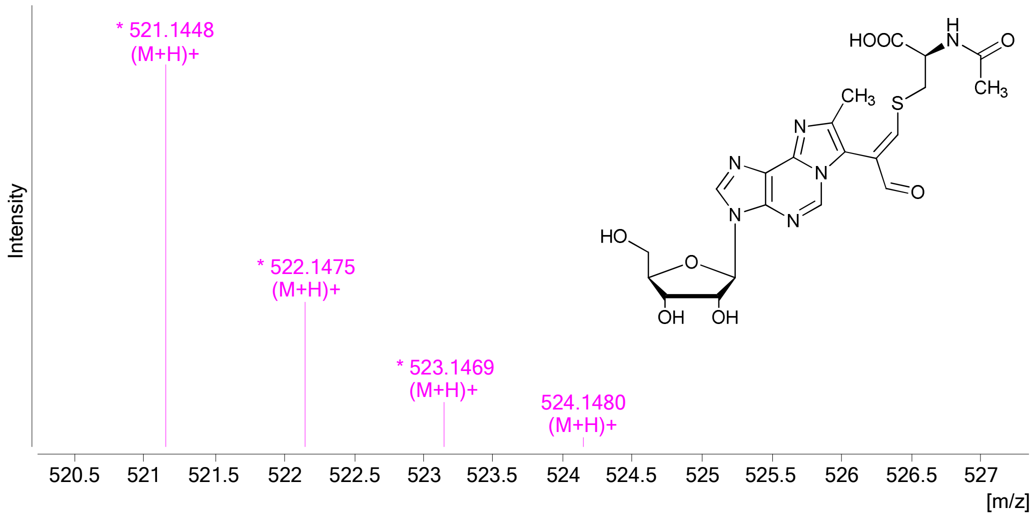

Fig. S18. Positive ions MS spectrum of M_1MGx-A-NAC

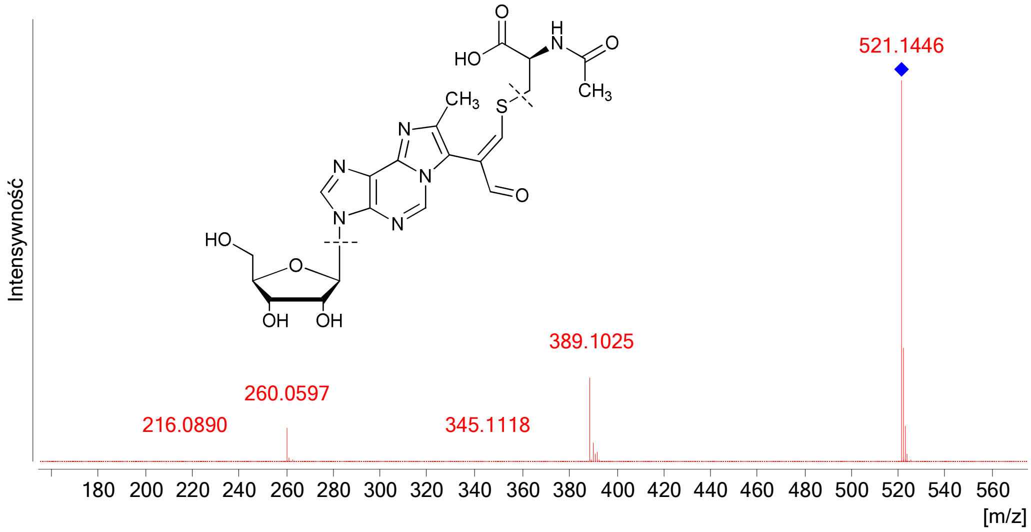

Fig. S19. Positive ions MS/MS spectrum of M_1MGx-A-NAC; collision energy 10 eV

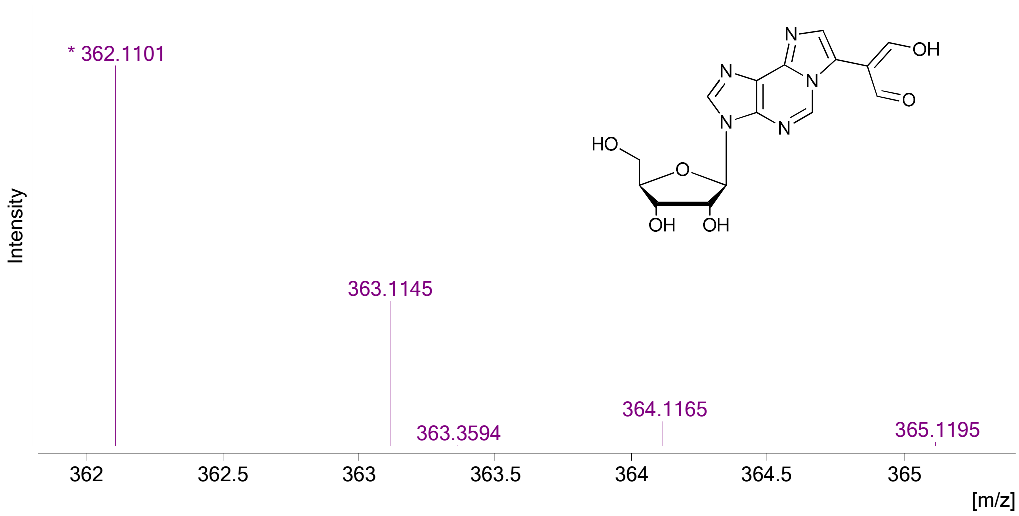

Fig. S20. Positive ions MS spectrum of M_1Gx-A

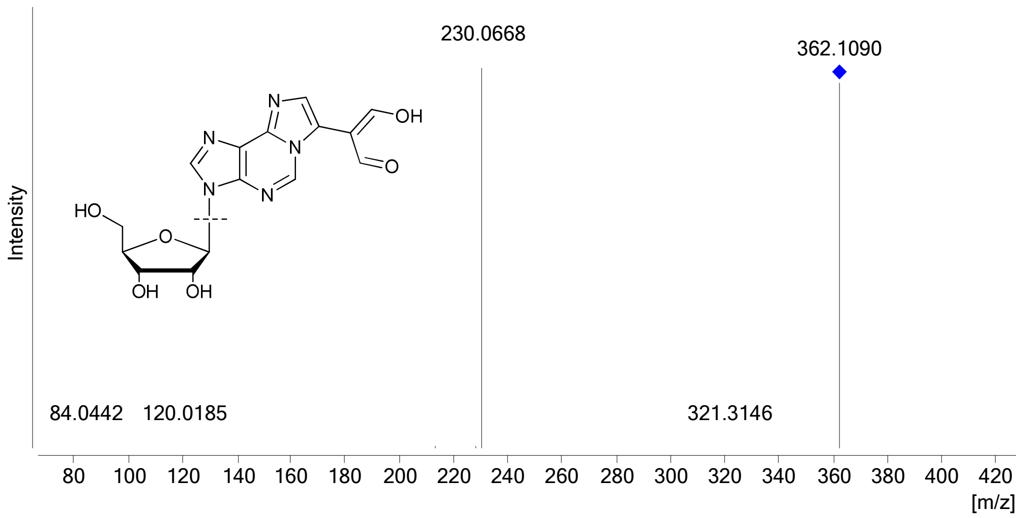

Fig. S21. Positive ions MS/MS spectrum of M_1Gx-A; collision energy 10 eV

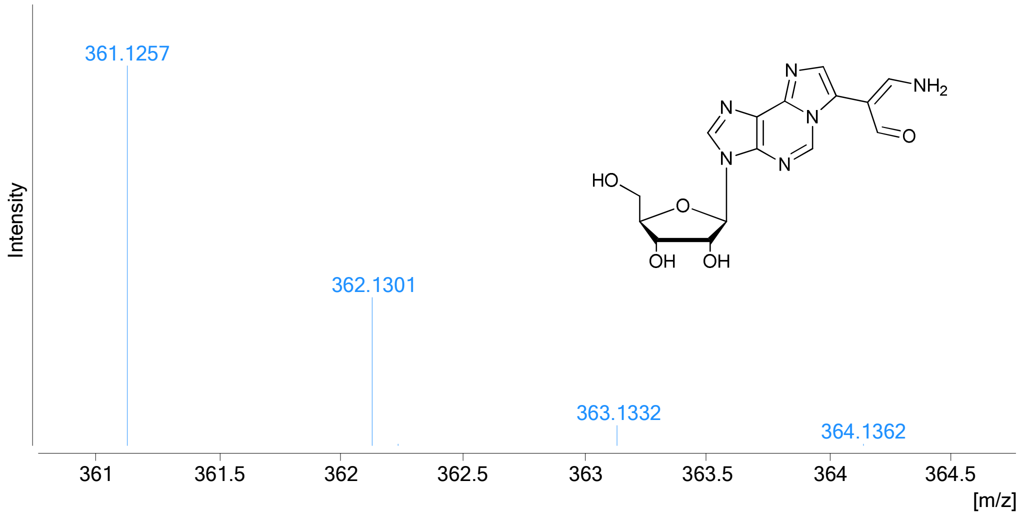

Fig. S22. Positive ions MS spectrum of $M_1Gx\text{-}A\text{-}NH_2$

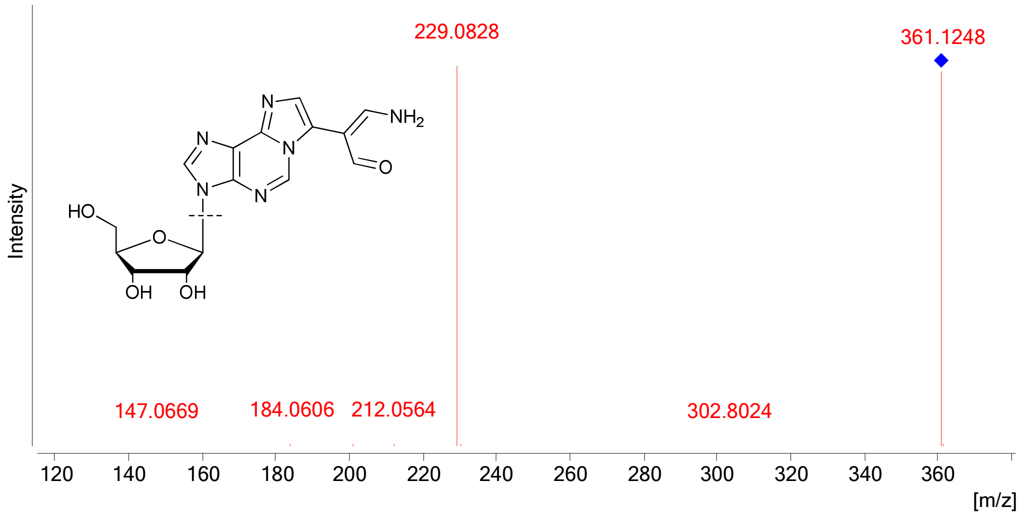

Fig. S23. Positive ions MS/MS spectrum of $M_1Gx\text{-}A\text{-}NH_2$; collision energy 10 eV

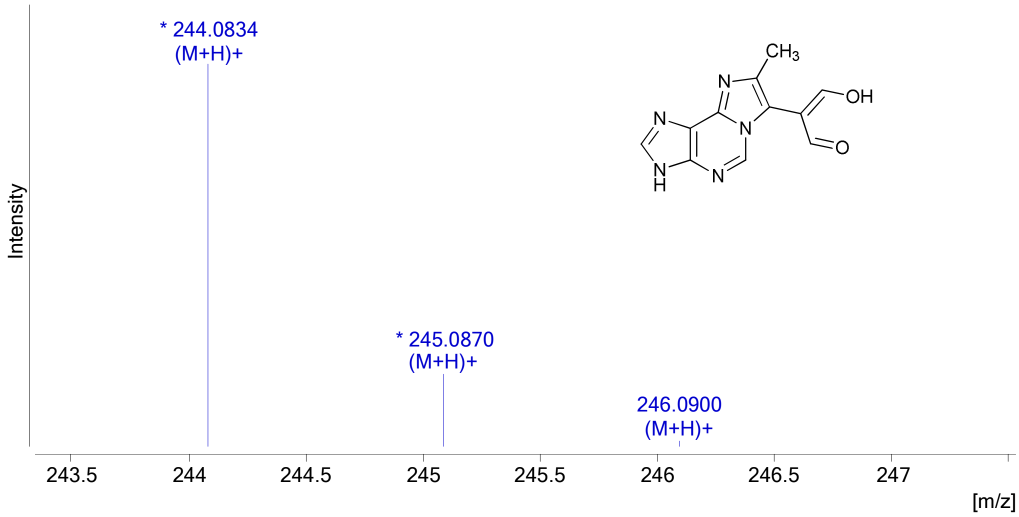

Fig. S24. Positive ions MS spectrum of $M_1MGx\text{-}Ade$

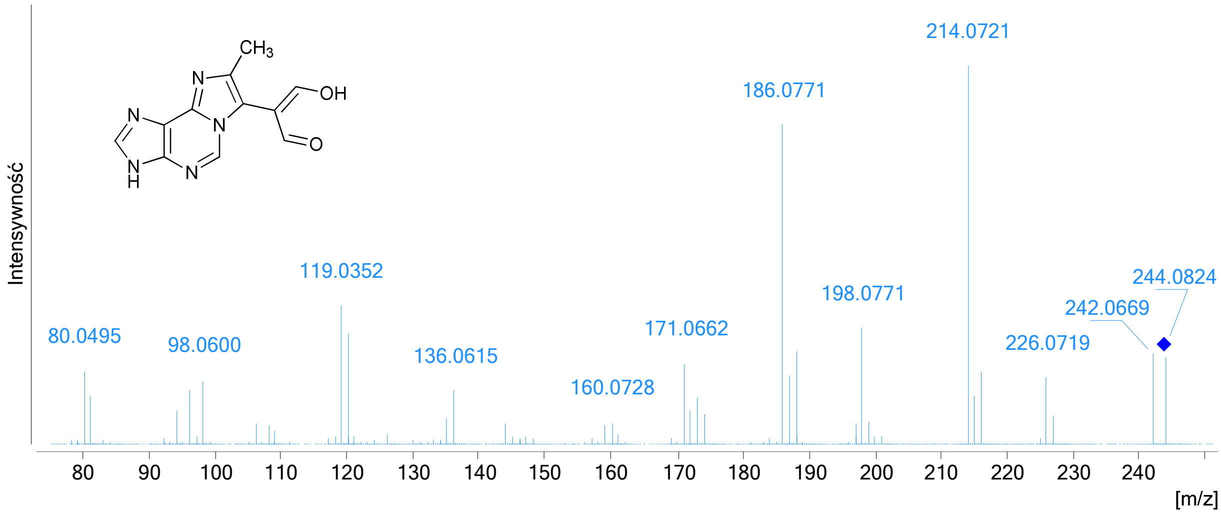

Fig. S25. Positive ions MS/MS spectrum of M_1MGx-Ade; collision energy 30 eV

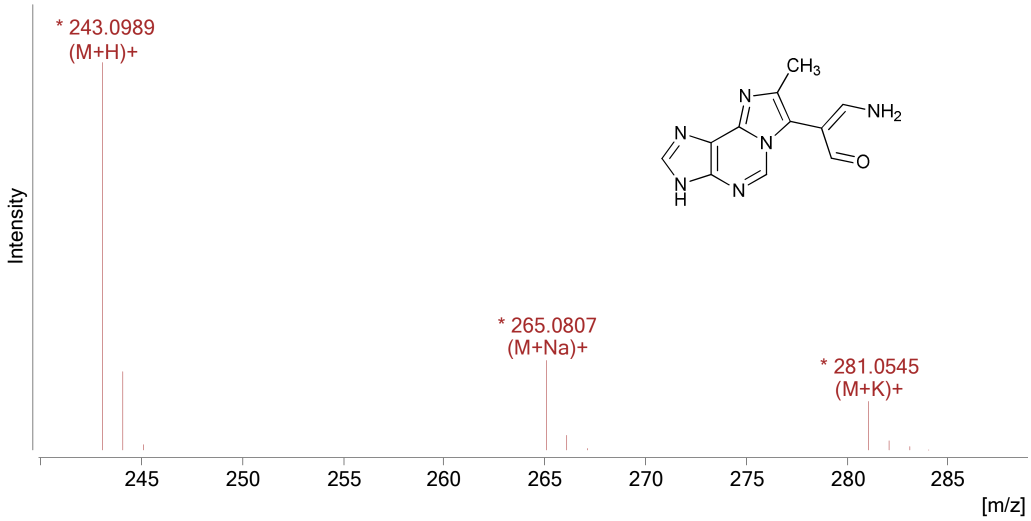

Fig. S26. Positive ions MS spectrum of M_1MGx-Ade-NH_2

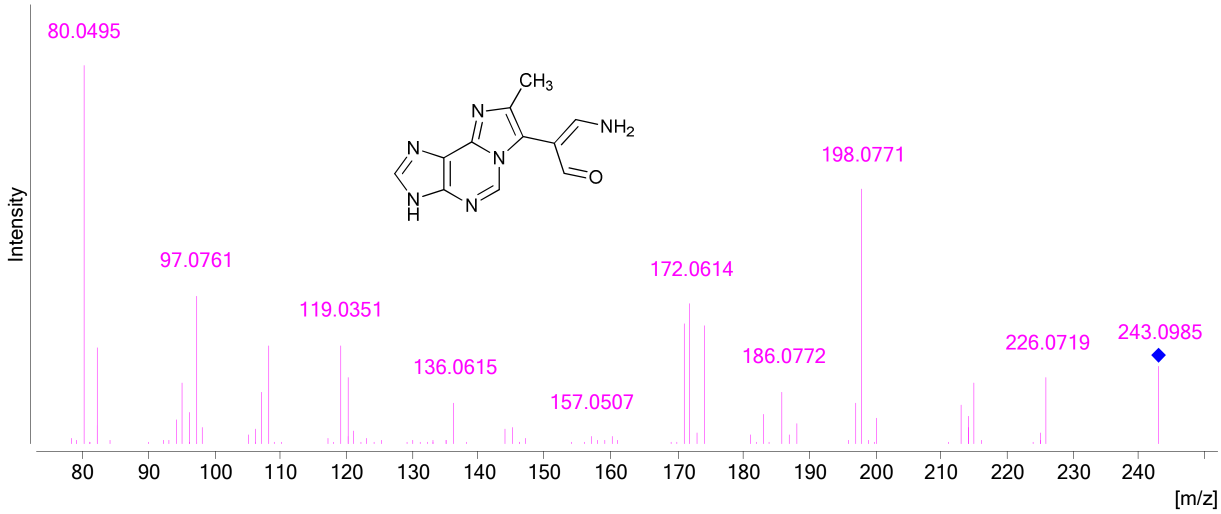

Fig. S27. Positive ions MS/MS spectrum of M_1MGx-Ade-NH_2; collision energy 30 eV

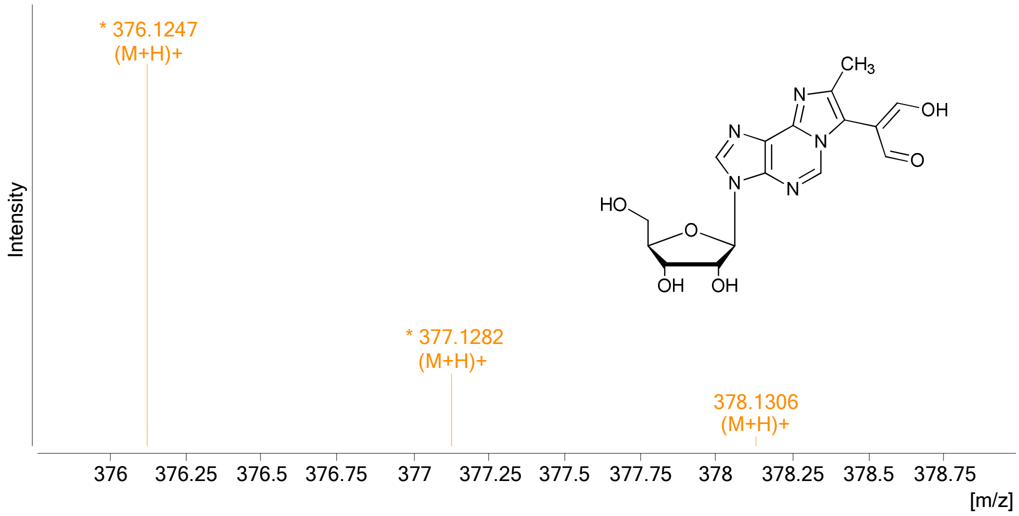

Fig. S28. Positive ions MS spectrum of M_1MGx-A

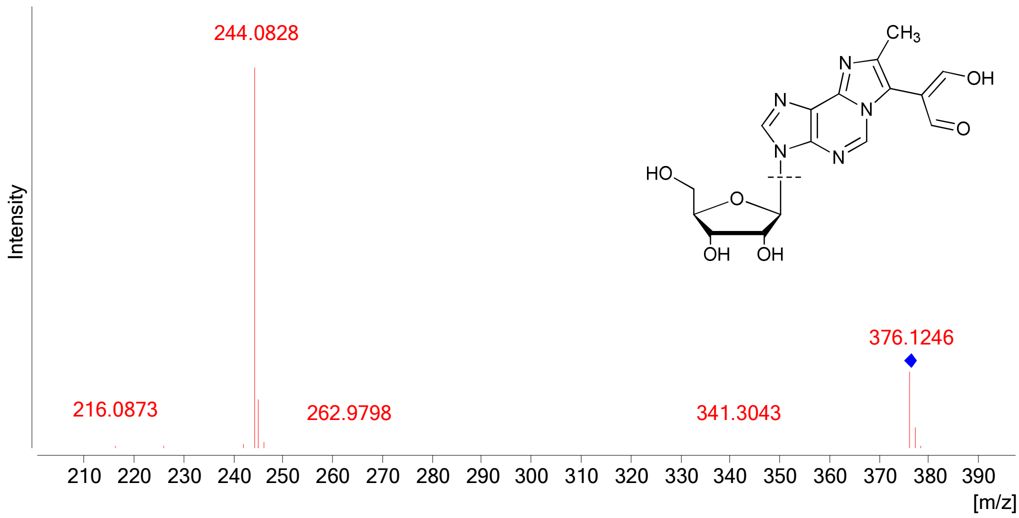

Fig. S29. Positive ions MS/MS spectrum of M_1MGx-A; collision energy 15 eV

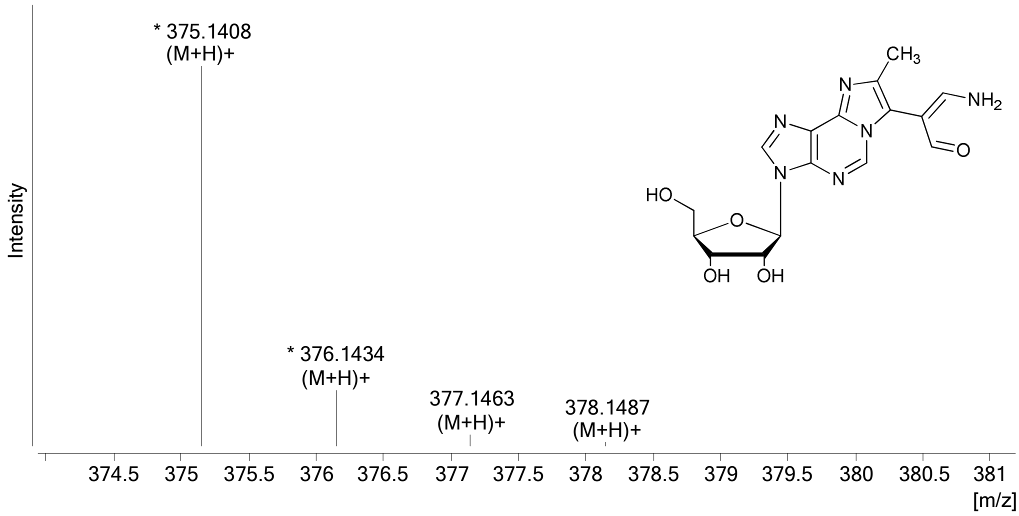

Fig. S30. Positive ions MS spectrum of M_1MGx-A-NH_2

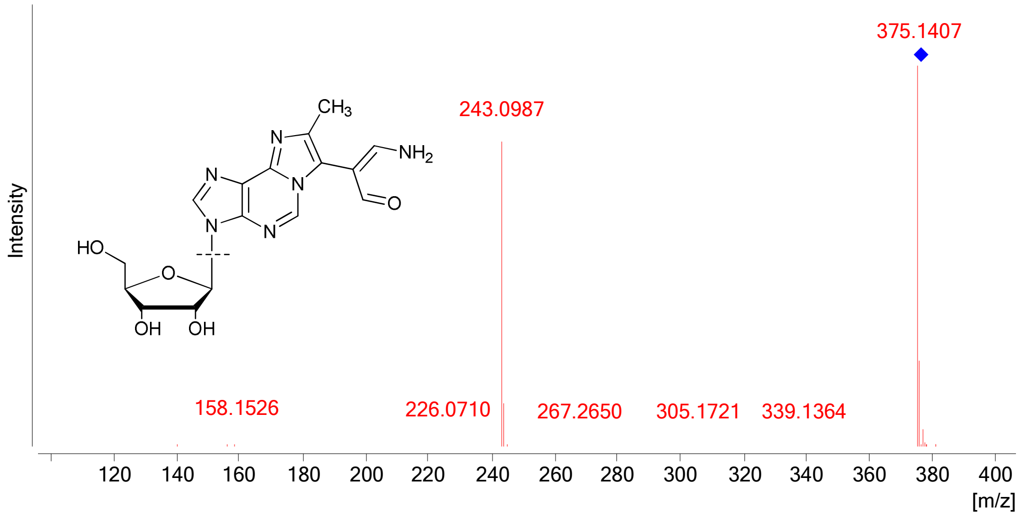

Fig. S31. Positive ions MS/MS spectrum of M_1MGx-A-NH_2; collision energy 10 eV

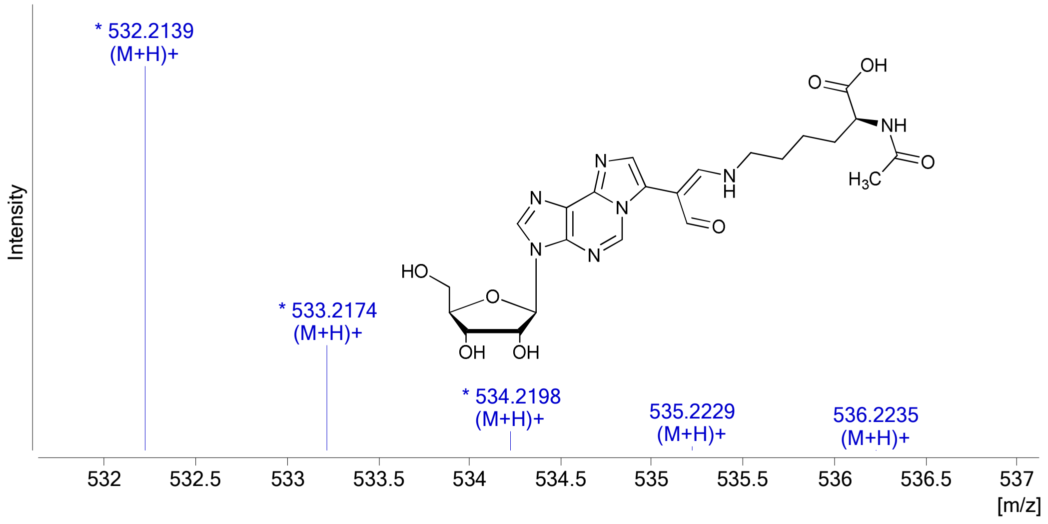

Fig. S32. Positive ions MS spectrum of M_1Gx-A-N^{α}AcLys

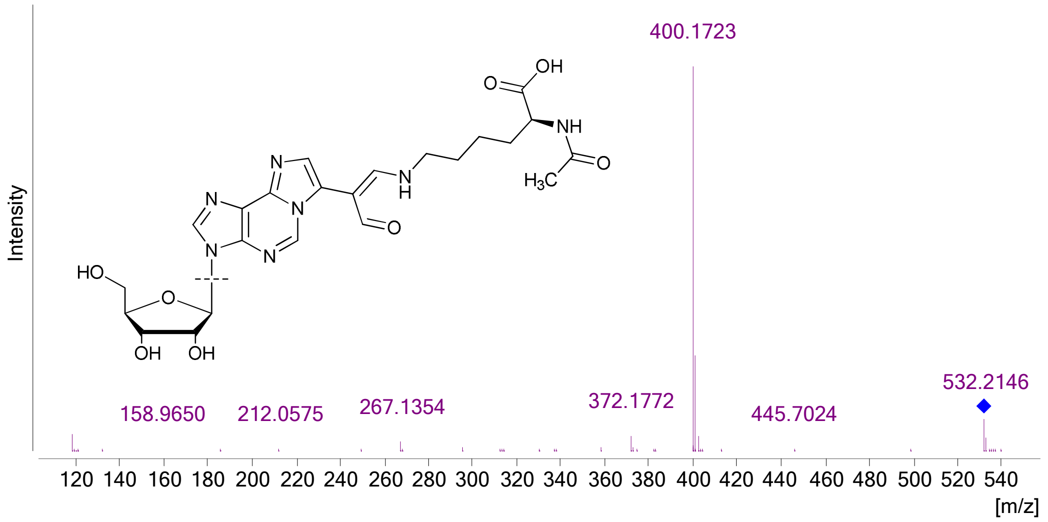

Fig. S33. Positive ions MS/MS spectrum of M_1Gx-A-N^{α}AcLys; collision energy 20 eV

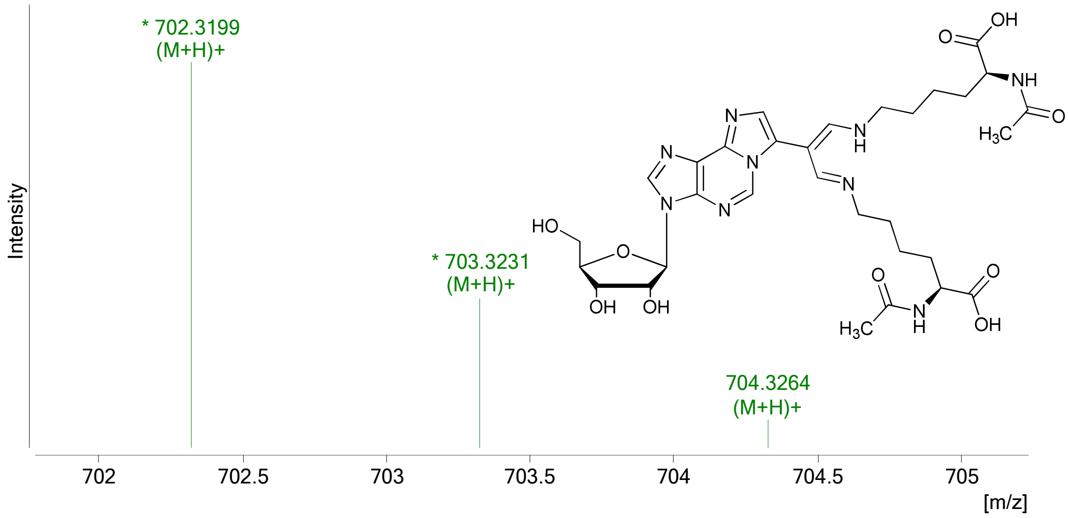

Fig. S34. Positive ions MS spectrum of M_1Gx-A-(N^{α}AcLys)$_2$

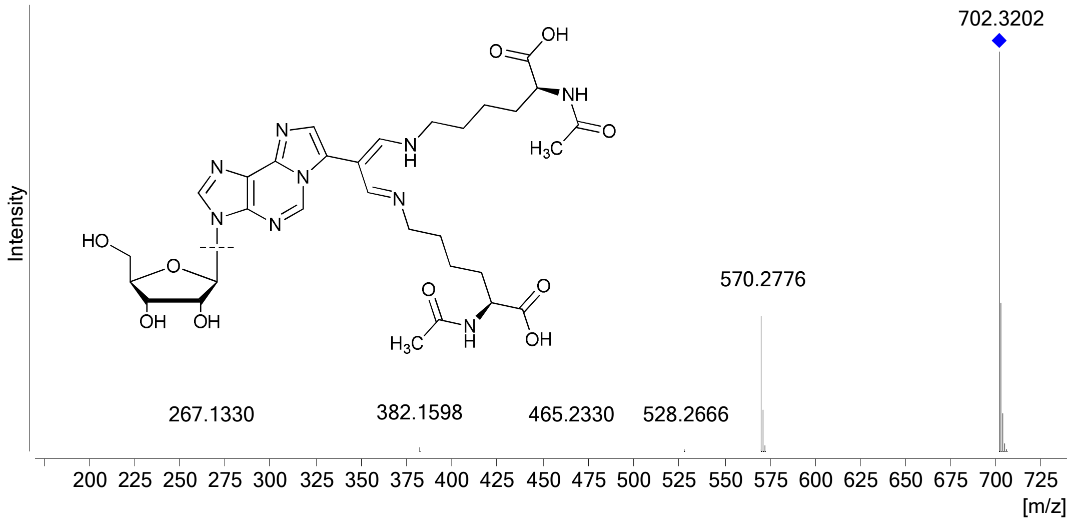

Fig. S35. Positive ions MS/MS spectrum of M_1Gx-A-(N^{α}AcLys)$_2$; collision energy 20 eV

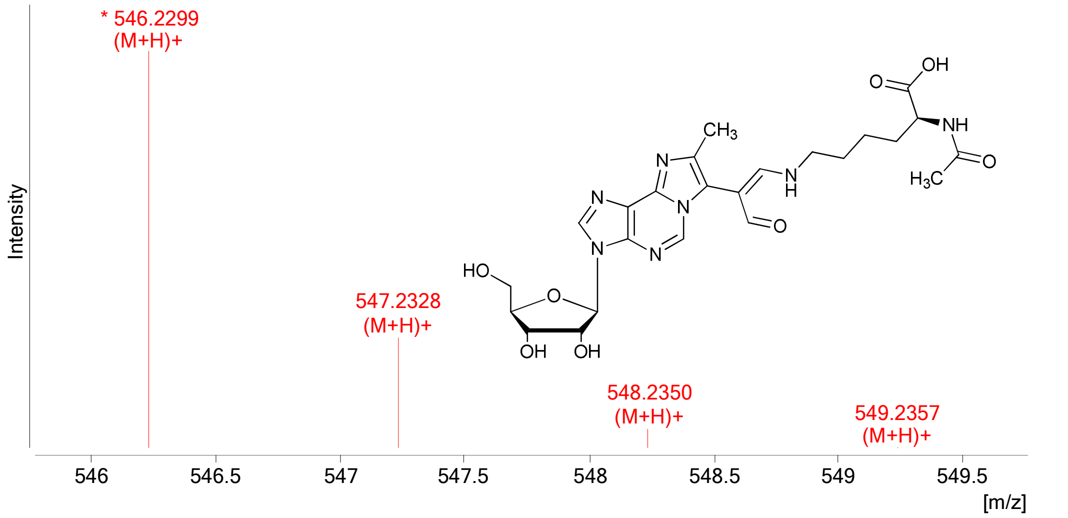

Fig. S36. Positive ions MS spectrum of M_1MGx-A-N^{α}AcLys

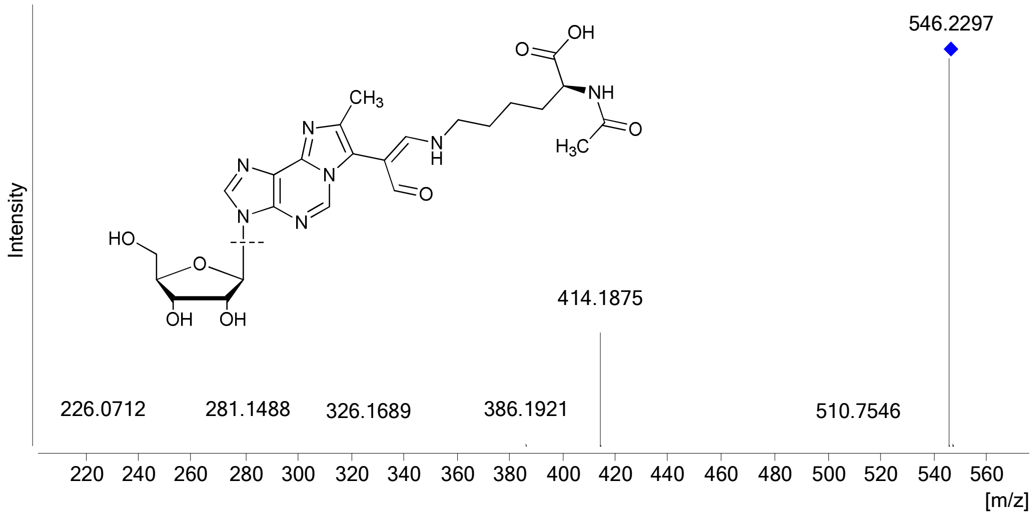

Fig. S37. Positive ions MS/MS spectrum of M$_1$MGx-A-N^{α}AcLys; collision energy 10 eV

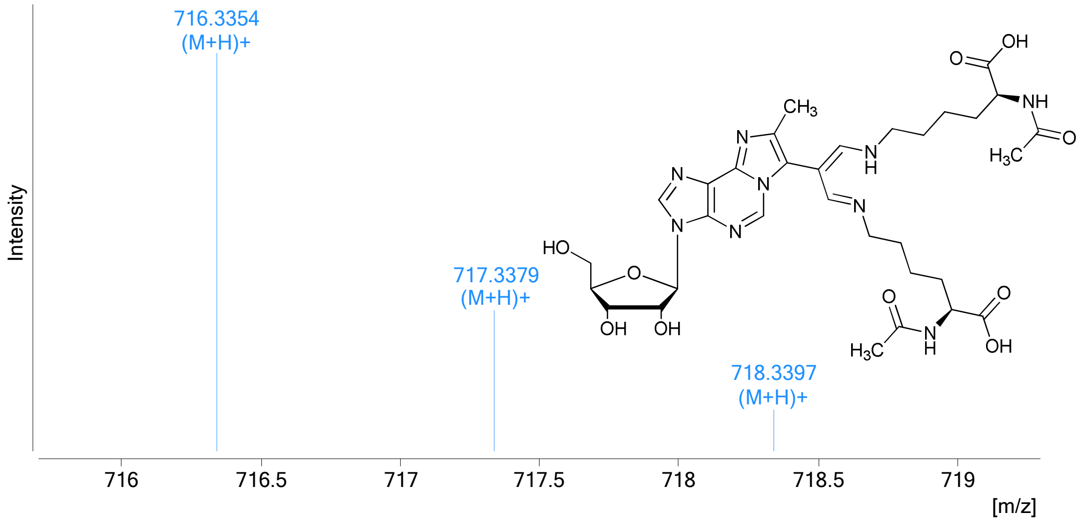

Fig. S38. Positive ions MS spectrum of M$_1$MGx-A-(N^{α}AcLys)$_2$

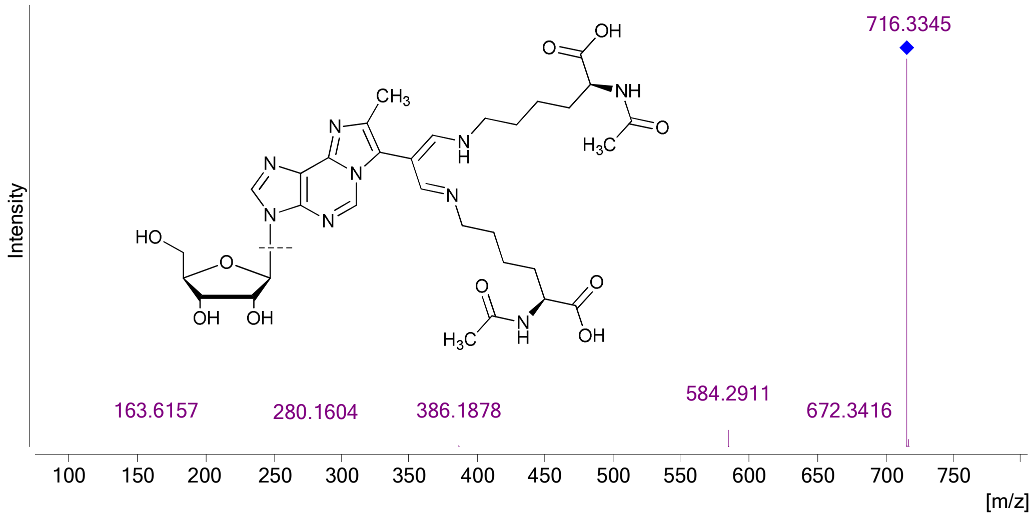

Fig. S39. Positive ions MS spectrum of M$_1$MGx-A-(N^{α}AcLys)$_2$; collision energy 10 eV

VT ^{1}H NMR spectra of M_1MGx-A-NAC

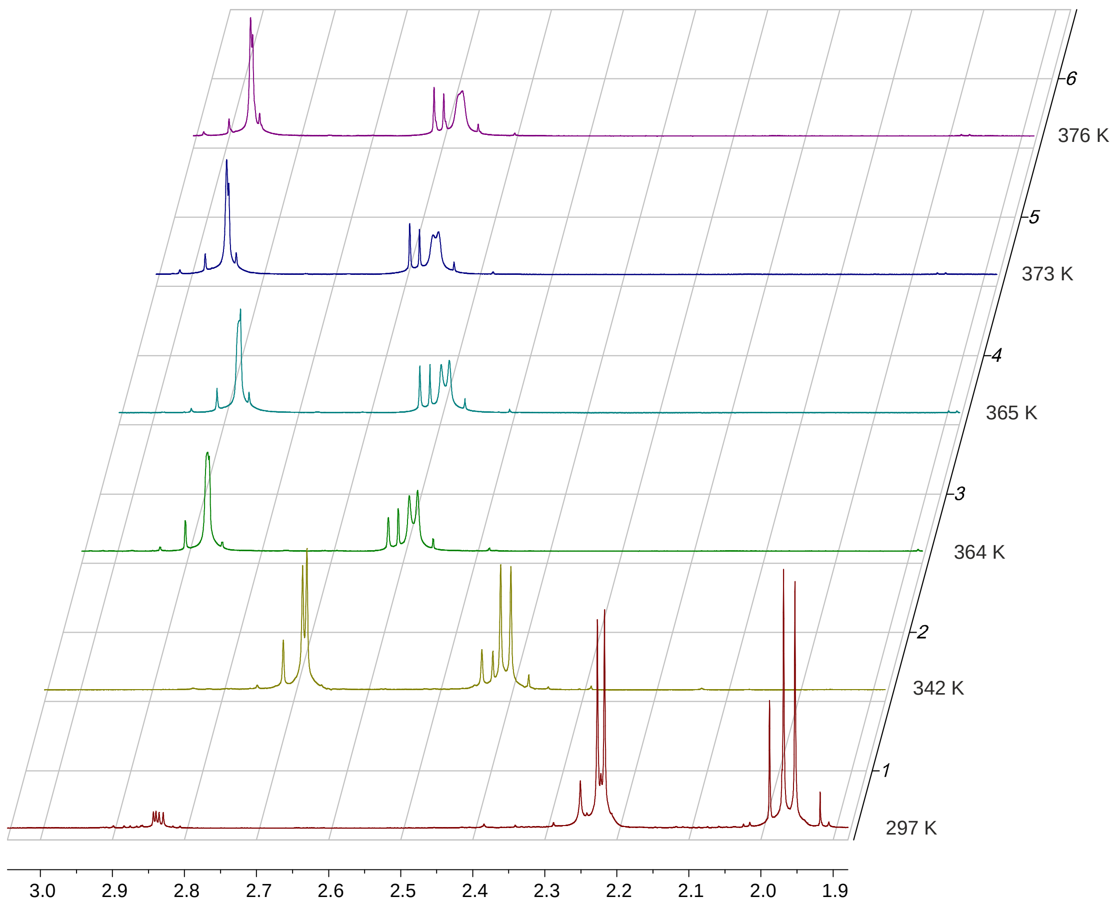

Fig. S40. Fragments of ^{1}H NMR spectra of M_1MGx-A-NAC (D_2O) recorded at 297 K, 342 K, 364, 365 K and 376. The split acetyl proton signals at 1.96 coalesced to singlet at Tc = 376 K, methyl protons signals at 2.23 ppm coalesced at lower temperature, but artefacts may be misleading. High temperature caused partial degradation of M_1MGx-A-NAC leading to the formation of products which gave rise to additional signals in ^{1}H NMR spectra of the studied compound. This process interfered with the variable-temperature studies.

Temperature calibration data

Table S2. Temperature values calculated based on [1]H NMR chemical shift values of hydroxyl and methylene protons of ethylene glycol

Thermostat temperature (T_t)	δ (–O<u>H</u>) [ppm]	δ (-C<u>H</u>$_2$) [ppm]	Δδ [ppm]	T_{calc}*
298	4.87	3.22	1.65	298.20
308	4.73	3.17	1.56	307.38
318	4.91	3.48	1.43	320.64
323	4.00	2.59	1.41	322.68
332	3.90	2.61	1.29	334.92
337	4.44	3.21	1.23	341.04
340	5.07	3.87	1.20	344.10
342	3.96	2.78	1.18	346.14

*Temperature values calculated based on $T_{calc} = 466.5 - 102.00 * \Delta\delta$

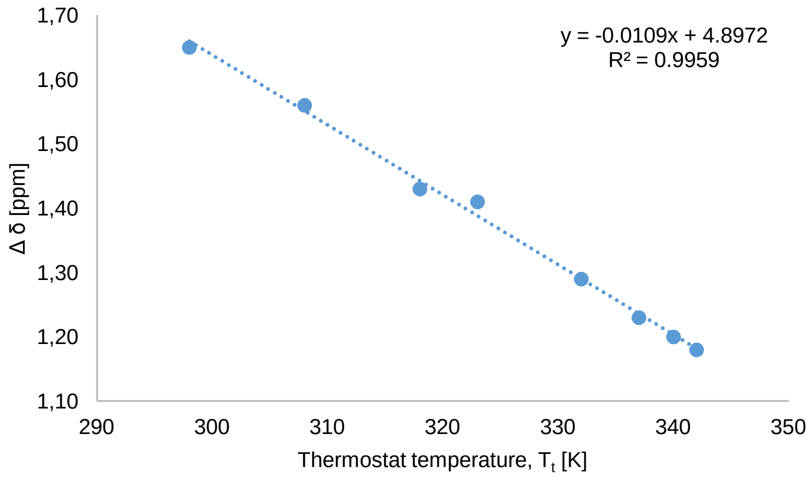

Chart S1. The relationship between [1]H NMR chemical shift difference values (Δδ) of ethylene glycol protons and temperature values showed by thermostat (T_t)

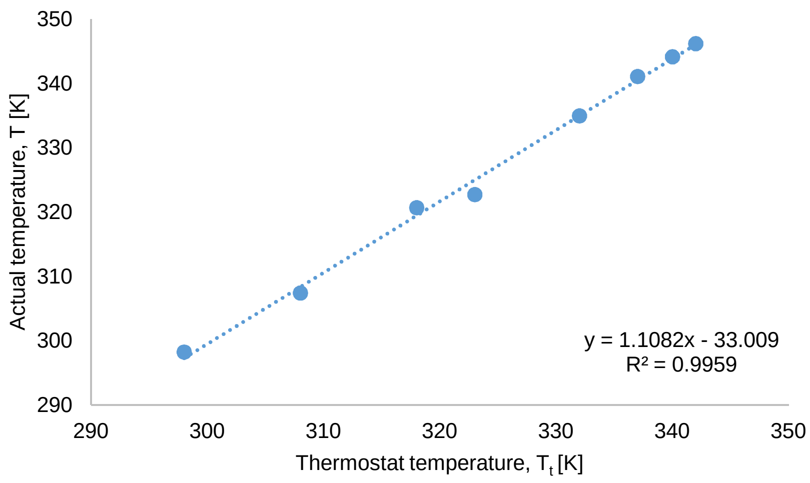

Chart S2. Calibration curve showing the relationship between thermostat temperature values (T_t) and calculated temperature (T_{calc}). Equation $T = 1.1082 * T_t – 33.009$ allows to determine the actual temperature in thermostat.

Quantum-chemical calculation results for M_1MGx-A-NAC

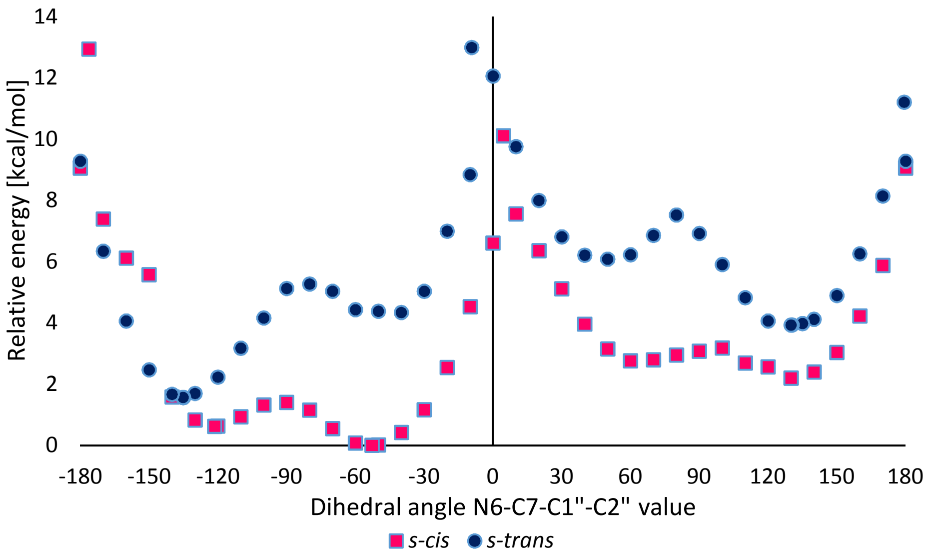

Chart S3. The relative energy of *s-cis* and *s-trans* conformers of M_1MGx-A-NAC dependent on the N6-C7-C1"-C2" dihedral angle value calculated at M06/6-31G(d) level of theory *in vacuo*

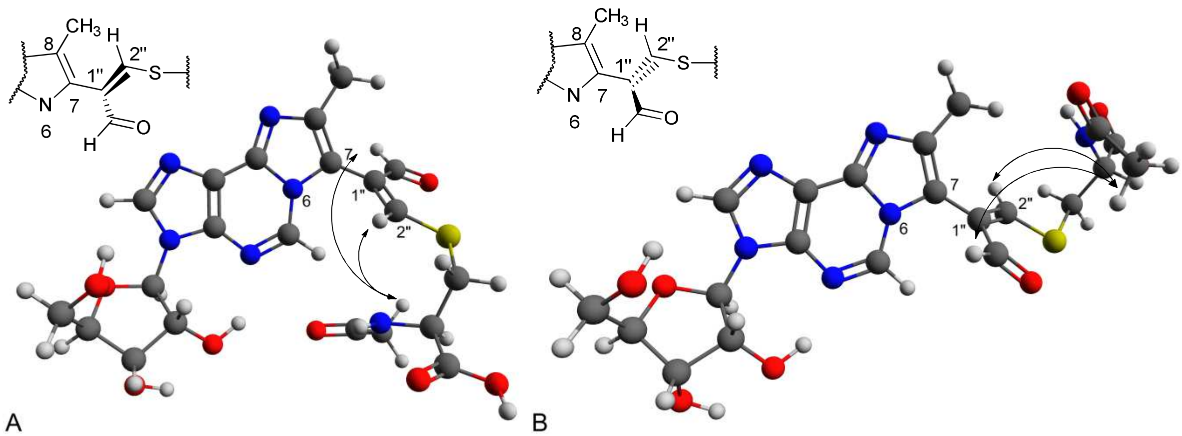

Fig. S41. Energy minima structures of M_1MGx-A-NAC: *s-cis*/M_{-50} (A) and *s-cis*/*P* (B); arrows show correlations observed in NOESY spectrum of M_1MGx-A-NAC (D_2O)

Table S3. Comparison of the relative energies (Δ*E*) and Gibbs free energies (Δ*G*) of M_1MGx-A-NAC *s-cis* and *s-trans* conformers calculated at M06/6-31G(d) level of theory *in vacuo*, and using PCM for water

	In vacuo			PCM (water)		
	Dihedral angle*	**Δ*E* [kcal/mol]**	**Δ*G* [kcal/mol]**	**Dihedral angle***	**Δ*E* [kcal/mol]**	**Δ*G* [kcal/mol]**
***s-cis*/*M*$_{-50}$**	**-52.8º**	0	0	**-54.4º**	0	0
***s-cis*/*M*$_{-120}$**	**-121.4º**	0.62	0.61	**-116.1º**	1.06	1.68
s-cis*/*P	**130.0º**	2.20	1.98	**129.5º**	1.80	1.44
***s-cis*/TS_0**	**4.5º**	10.12	12.01	**2.7º**	11.05	12.66
***s-cis*/TS _180**	**-176.3º**	12.95	13.90	**-174.1º**	12.58	13.67
s-trans*/*M	**-135.2º**	1.57	1.68	**-128.9º**	1.72	2.42
s-trans*/*P	**130.5º**	3.93	2.94	**128.8º**	2.48	3.36
***s-trans*/TS_0**	**-9.3º**	13.00	12.03	**-6.4º**	16.36	16.90
***s-trans*/TS _180**	**179.3º**	11.21	12.07	**178.0º**	11.47	12.87

* N6-C7-C1”-C2” dihedral angle value

Table S4. The relative energy values (Δ*E*) of *s-cis* and *s-trans* conformers of M_1MGx-A-NAC calculated using M06/6-31++G(d,p), B3LYP/6-31++G(d,p), ωB97X-D/6-31G(d) and MP2/6-31G(d) *in vacuo*. For comparison the Δ*E* values calculated at initial M06/6-31G(d) level were given.

	Dihedral angle*	**M06/ 6-31G(d)**	**M06/ 6-31++G(d,p)**	**B3LYP/ 6-31++G(d,p)**	**ωB97X-D/ 6-31G(d)**	**MP2/ 6-31G(d)**
***s-cis*/*M*$_{-50}$**	**-52.8º**	0.00	0.00	0.00	0.00	0.04
s-cis*/*P	**130.0º**	2.20	1.74	1.53	2.81	3.06
***s-cis*/TS_0**	**4.5º**	10.12	9.72	9.41	11.35	13.73
***s-cis*/TS _180**	**-176.3º**	12.95	12.42	13.04	14.83	20.11
s-trans*/*M	**-135.2º**	1.57	0.83	1.71	1.41	0.00
s-trans*/*P	**130.5º**	3.93	3.42	3.89	4.15	2.82
***s-trans*/TS_0**	**-9.3º**	13.00	12.01	12.09	13.04	11.42
***s-trans*/TS _180**	**179.3º**	11.21	10.91	11.49	12.27	14.51

* N6-C7-C1”-C2” dihedral angle value

Transition state structures of M_1MGx-Ade-NAC

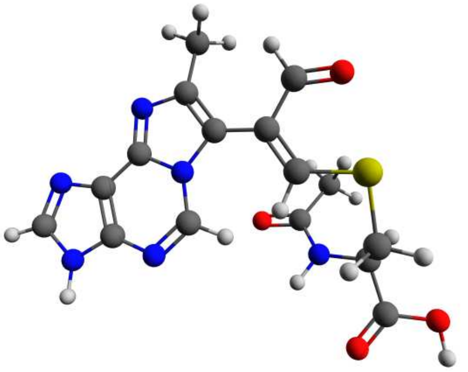

***s-cis*/TS_0**

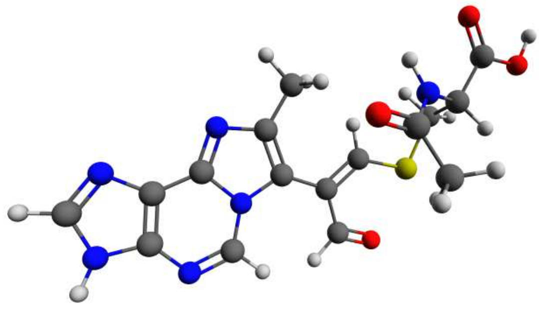

***s-cis/*TS_180**

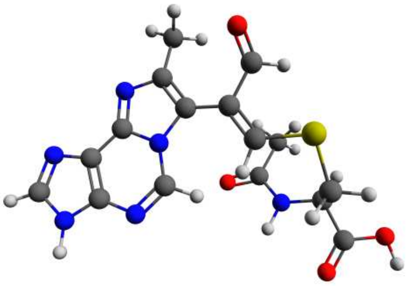

***s-trans*/TS_0**

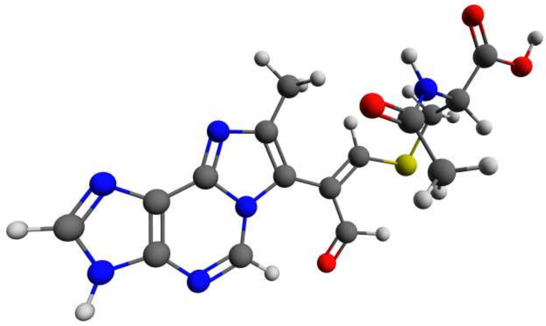

***s-trans*/TS_180**

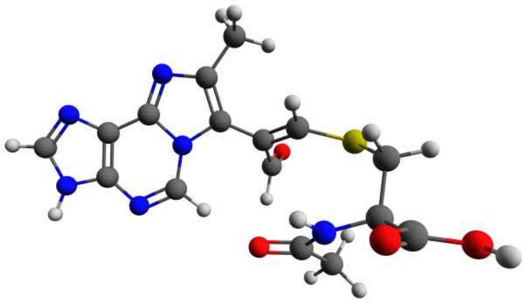

***M*/TS_-90**

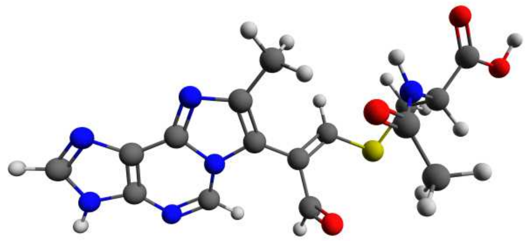

***P*/TS_90**

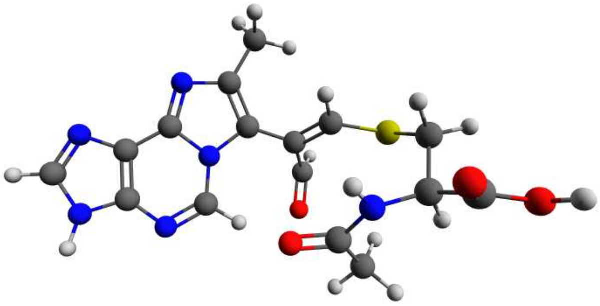

***M*/TS_90**

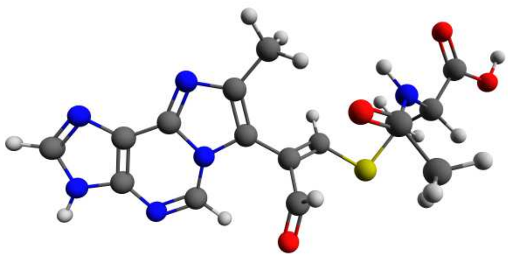

***P*/TS_-90**

Fig. S42. Transition state structures of M_1MGx-Ade-NAC calculated at M06/6-31G(d) level of theory *in vacuo*

NMR spectra

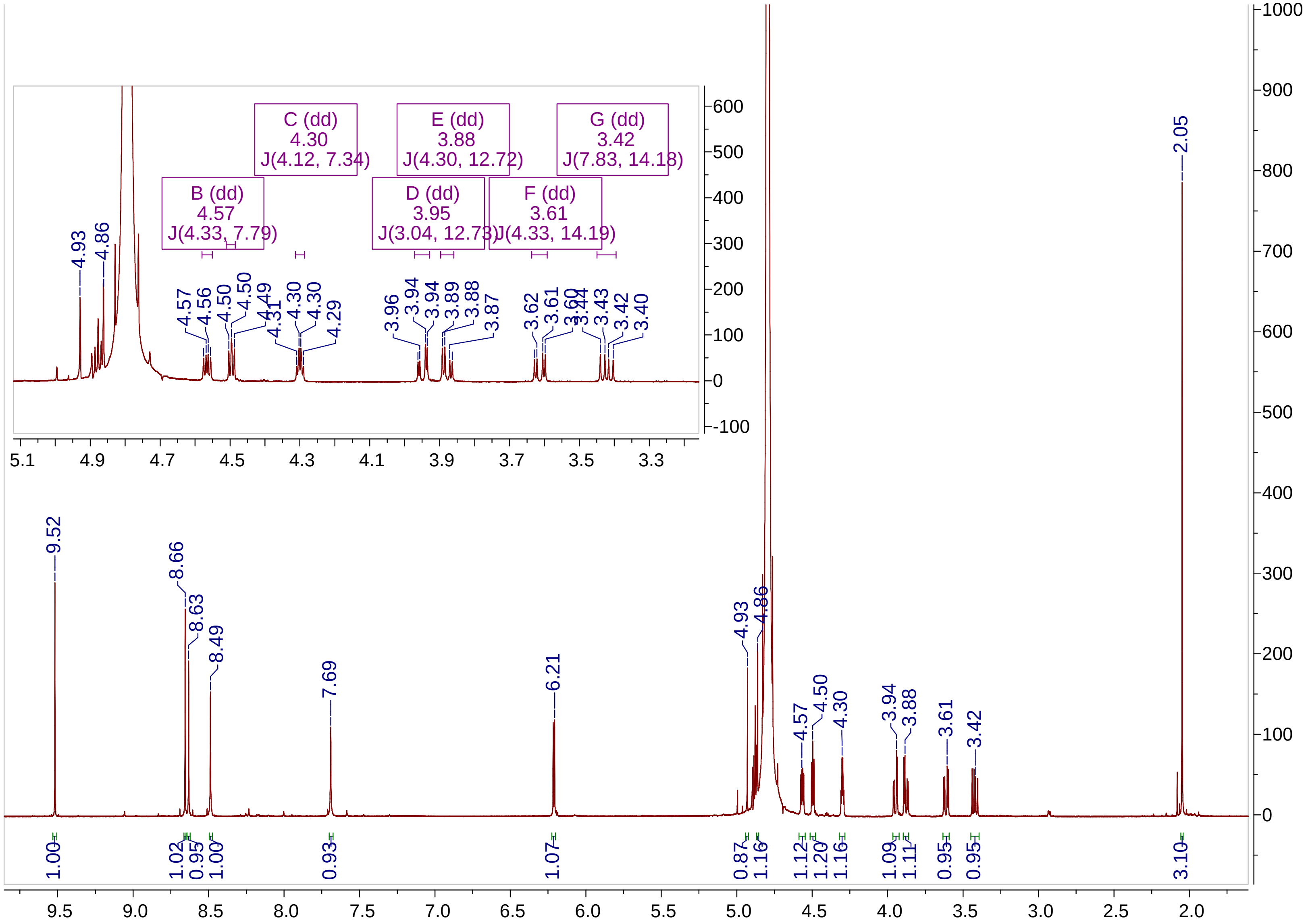

Fig. S43. **^{1}H NMR spectrum of M_1Gx-A-NAC (D_2O)**

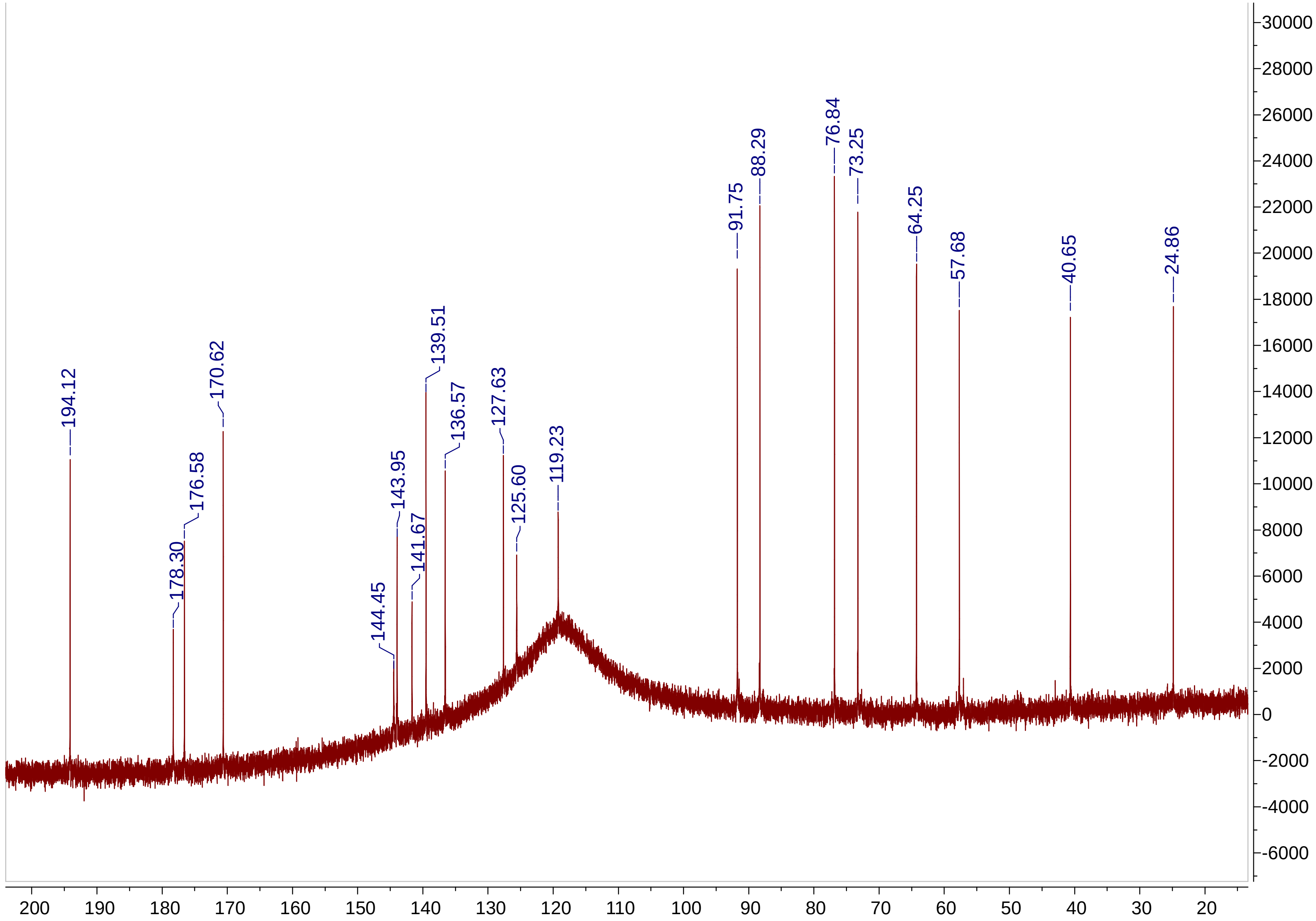

Fig. S44. ^{13}**C NMR spectrum of** M_1**Gx-A-NAC (**D_2O**)**

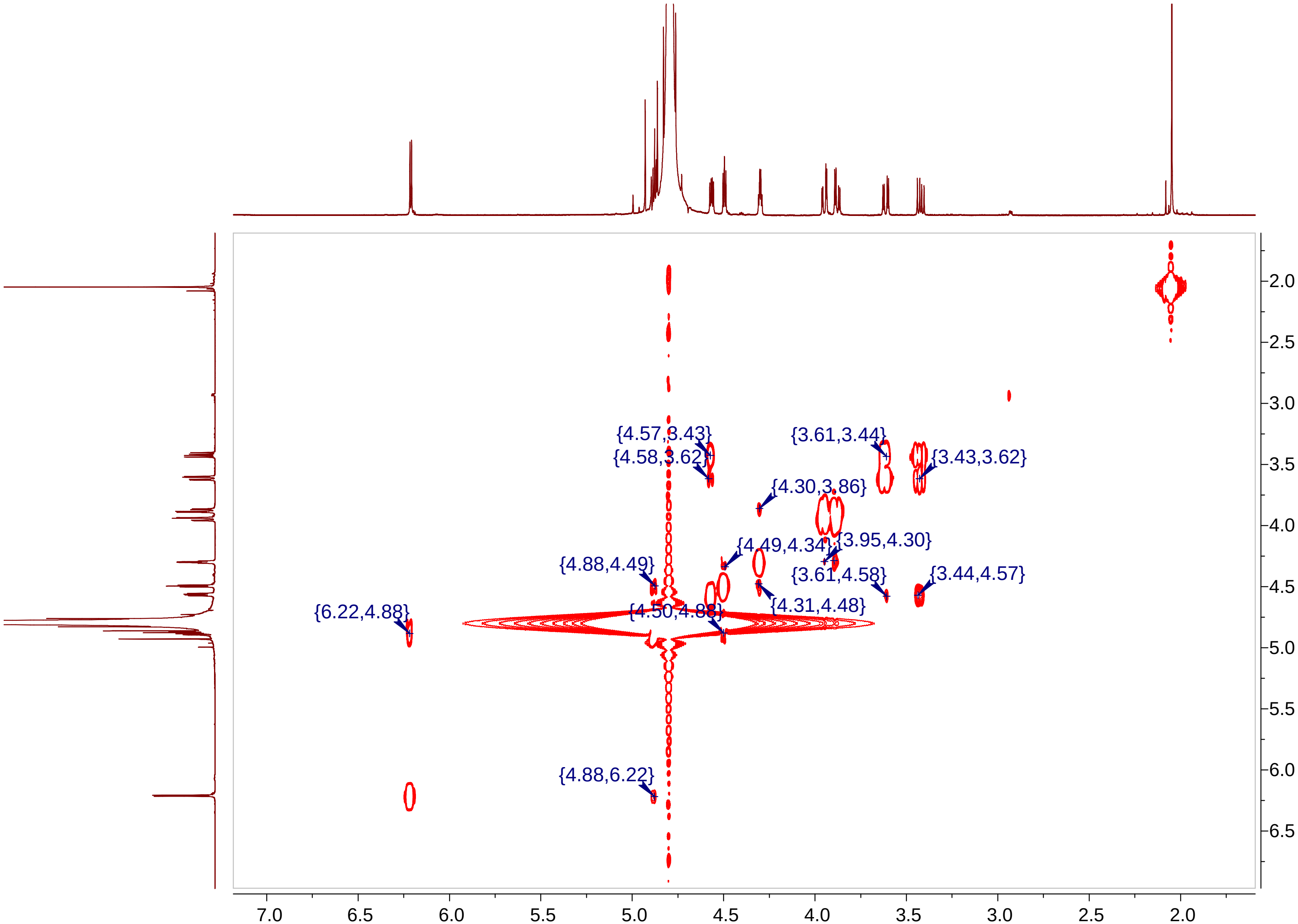

Fig. S45. COSY spectrum of M_1Gx-A-NAC (D_2O)

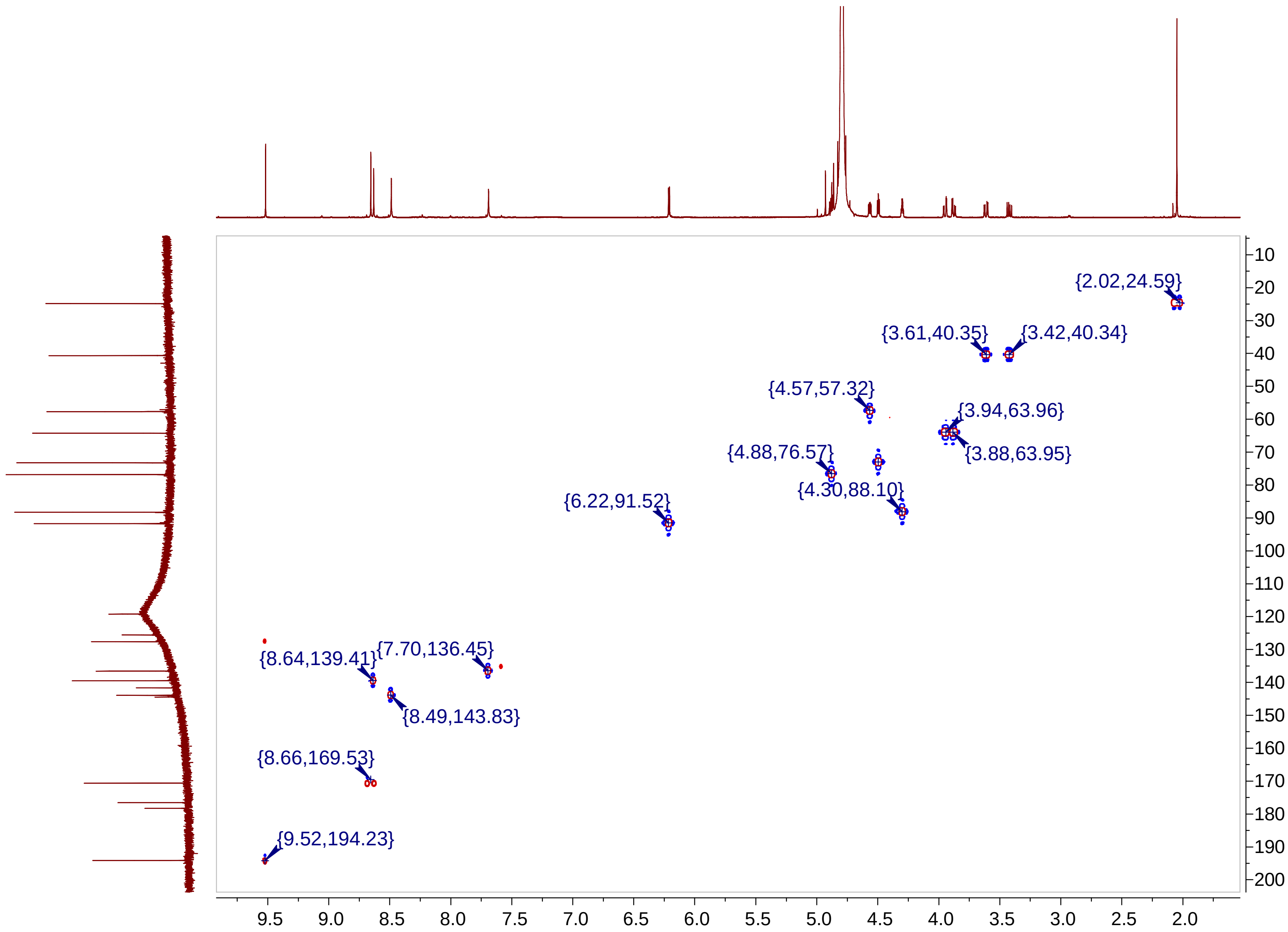

Fig. S46. HSQC spectrum of M_1Gx-A-NAC (D_2O)

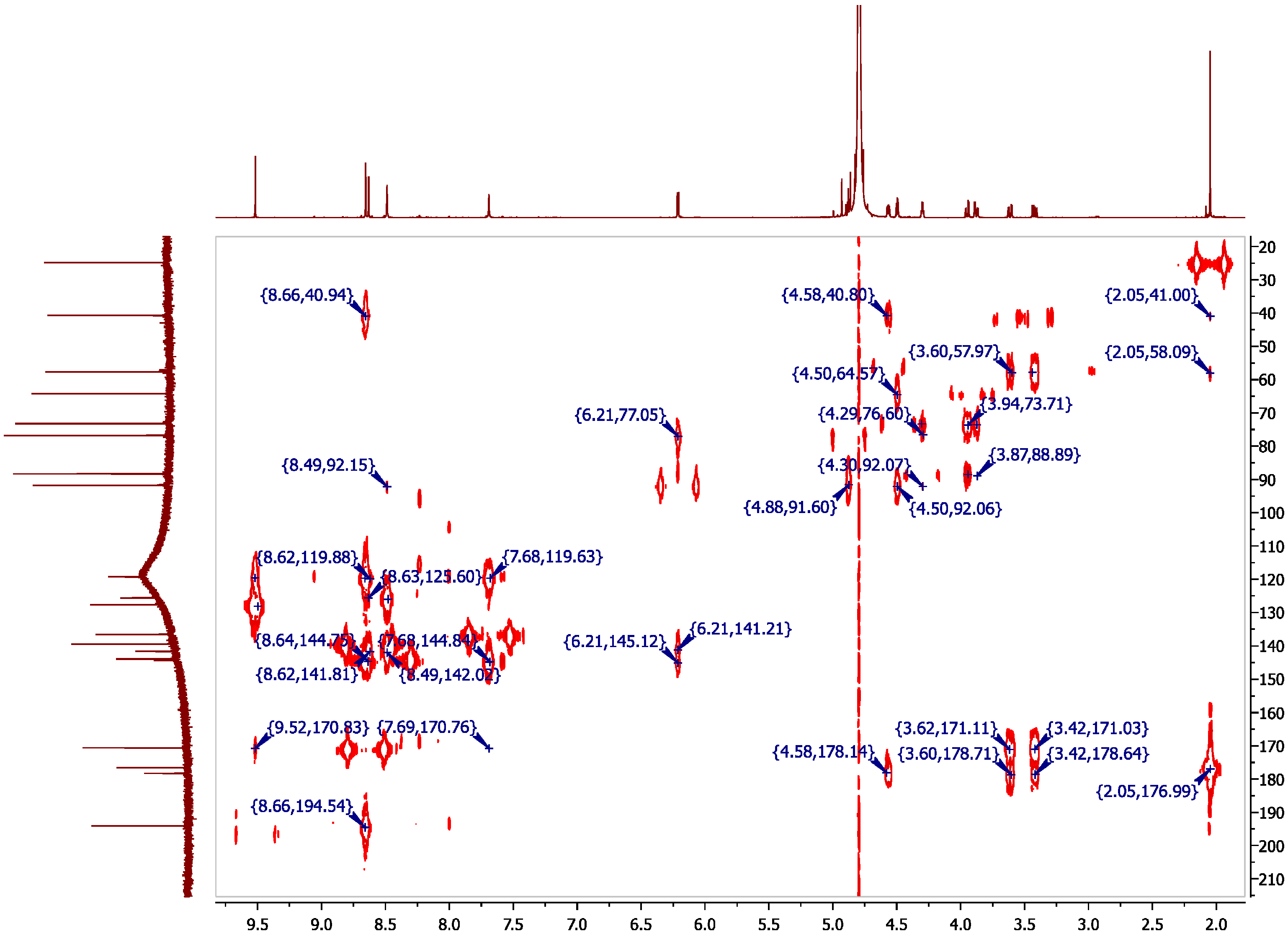

Fig. S47. HMBC spectrum of M_1Gx-A-NAC (D_2O)

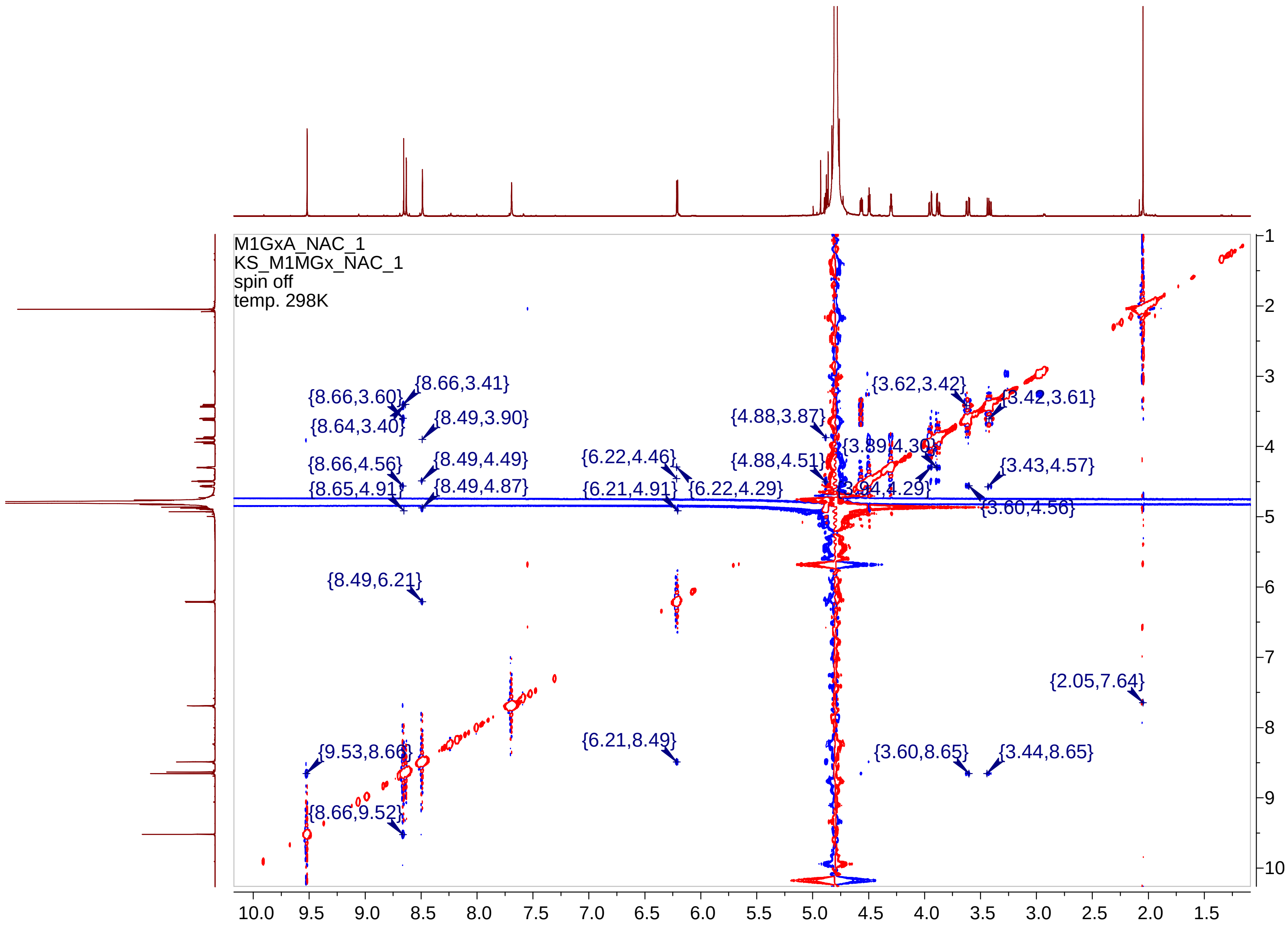

Fig. S48. NOESY spectrum of M_1Gx-A-NAC (D_2O)

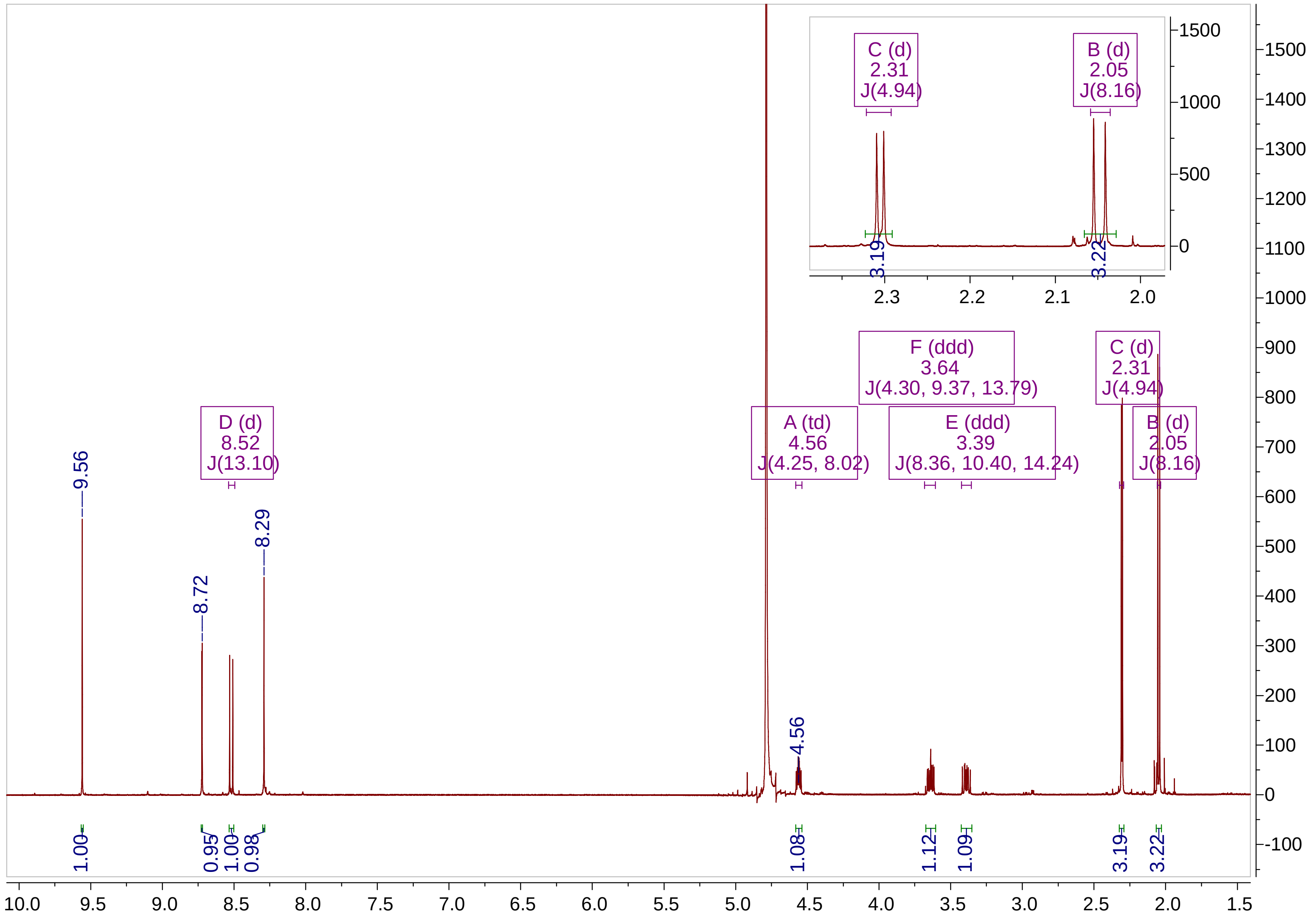

Fig. S49. ^{1}**H NMR spectrum of M**$_1$**MGx-Ade-NAC (D**$_2$**O)**

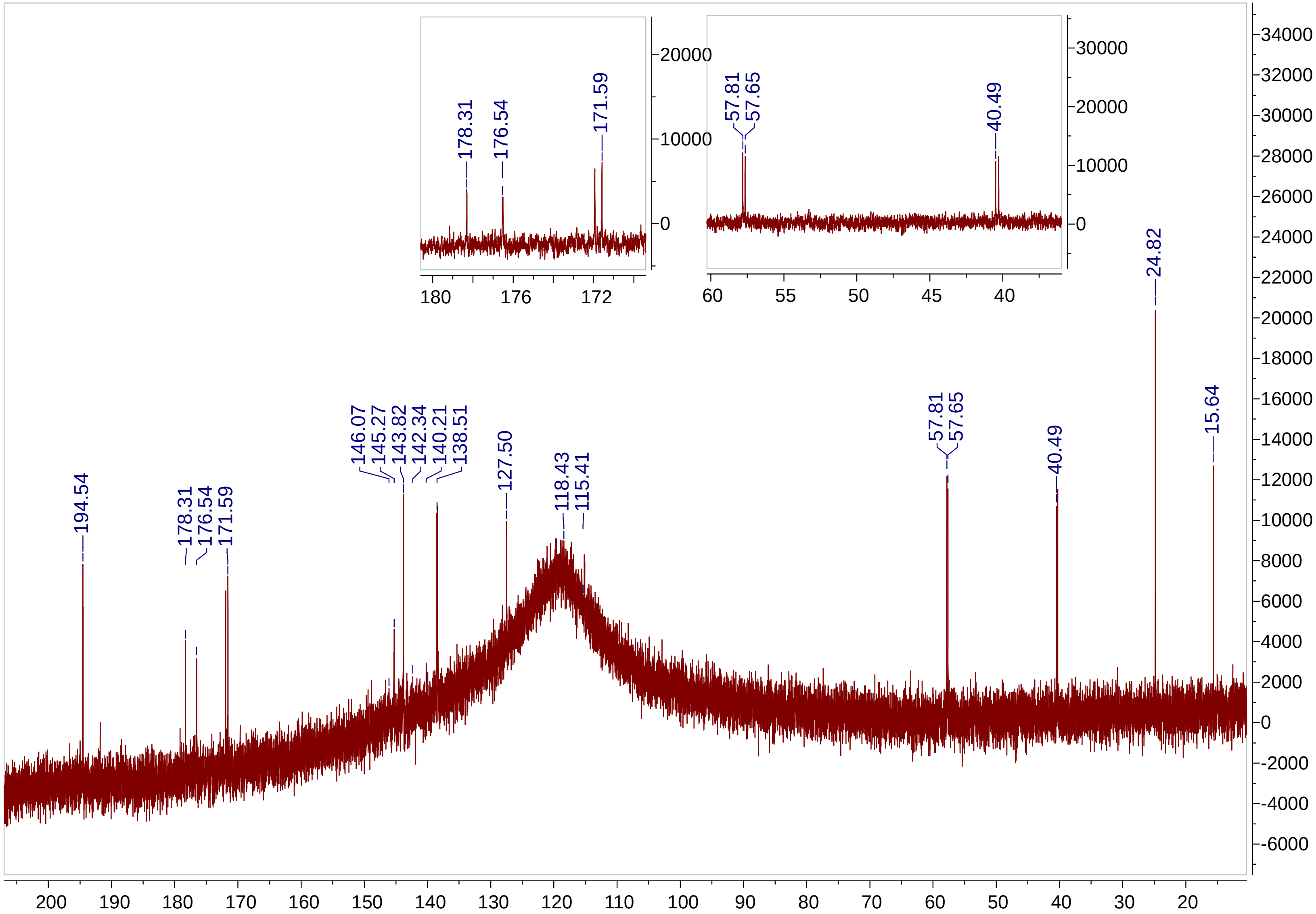

Fig. S50. ^{13}**C NMR spectrum of** M_1**MGx-Ade-NAC (**D_2O**)**

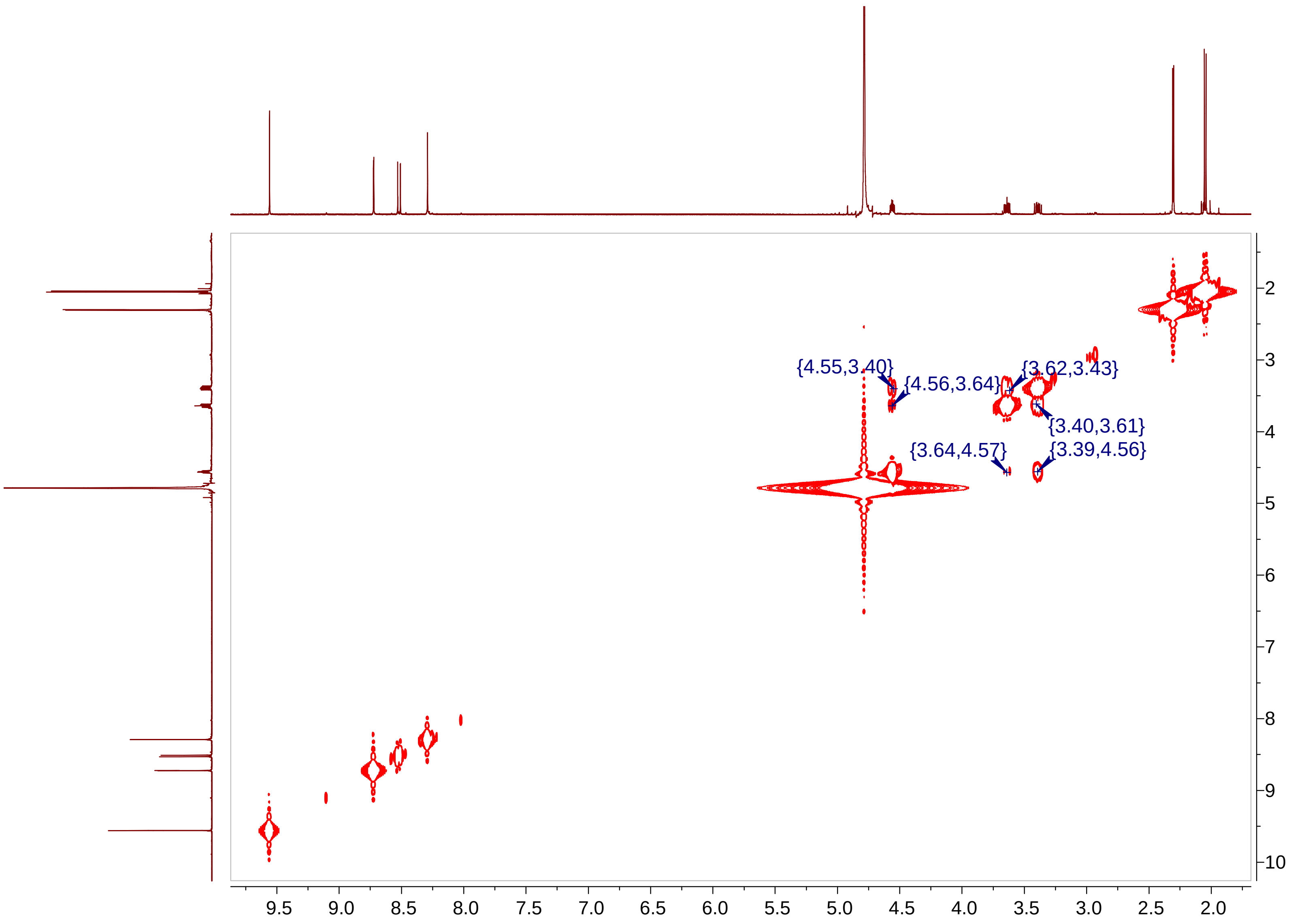

Fig. S51. COSY spectrum of M_1MGx-Ade-NAC (D_2O)

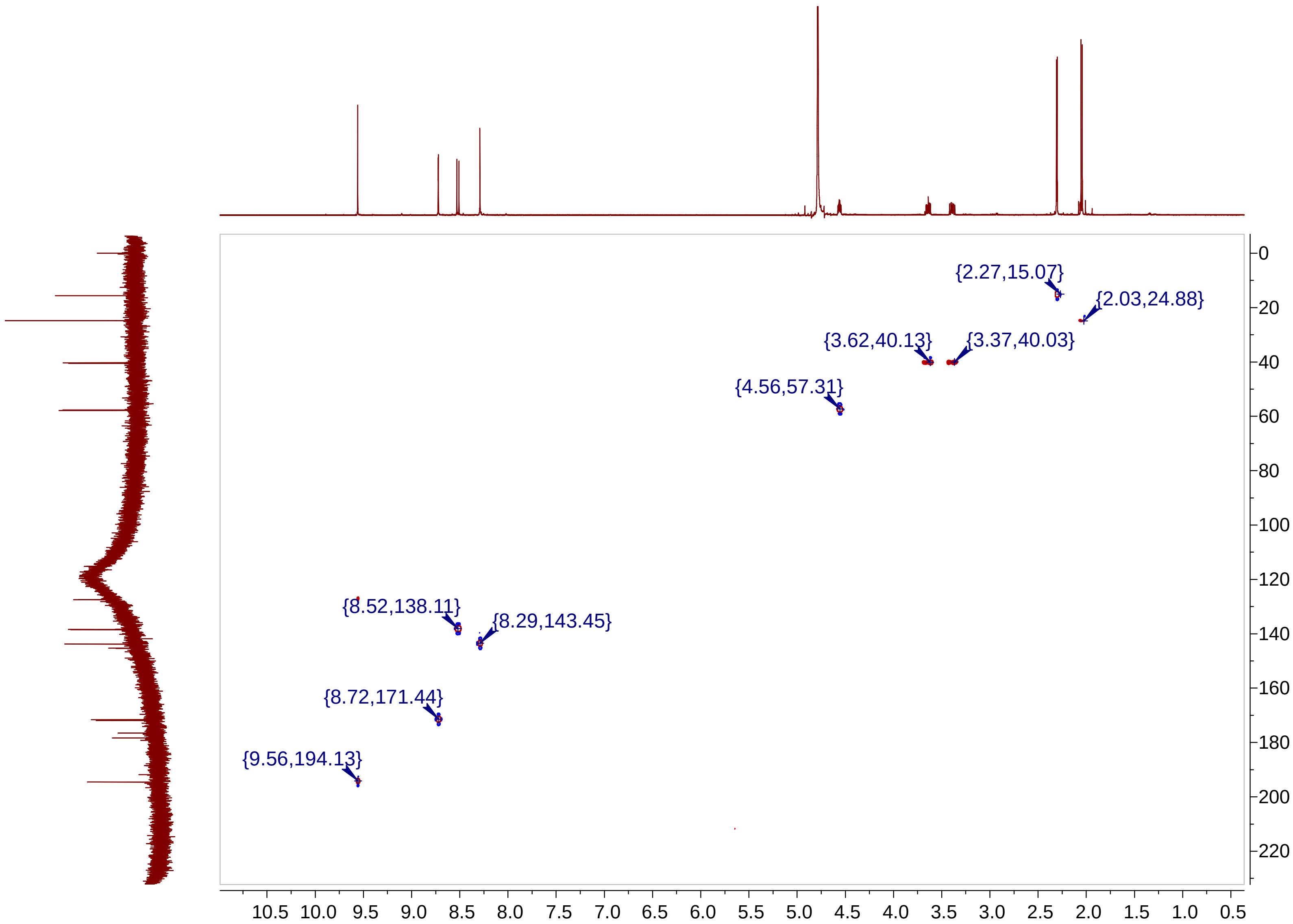

Fig. S52. HSQC spectrum of M_1MGx-Ade-NAC (D_2O)

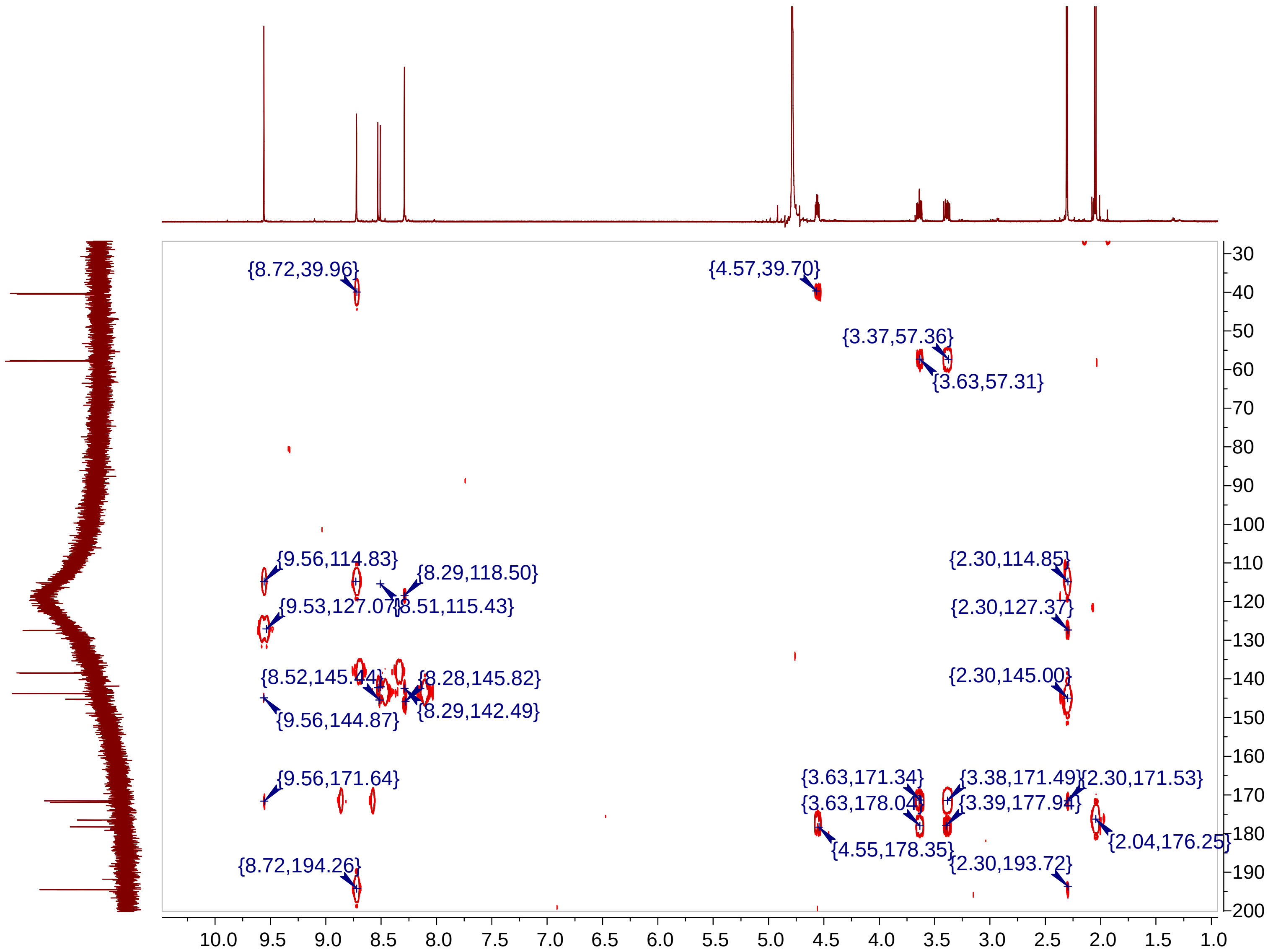

Fig. S53. HMBC spectrum of M_1MGx-Ade-NAC (D_2O)

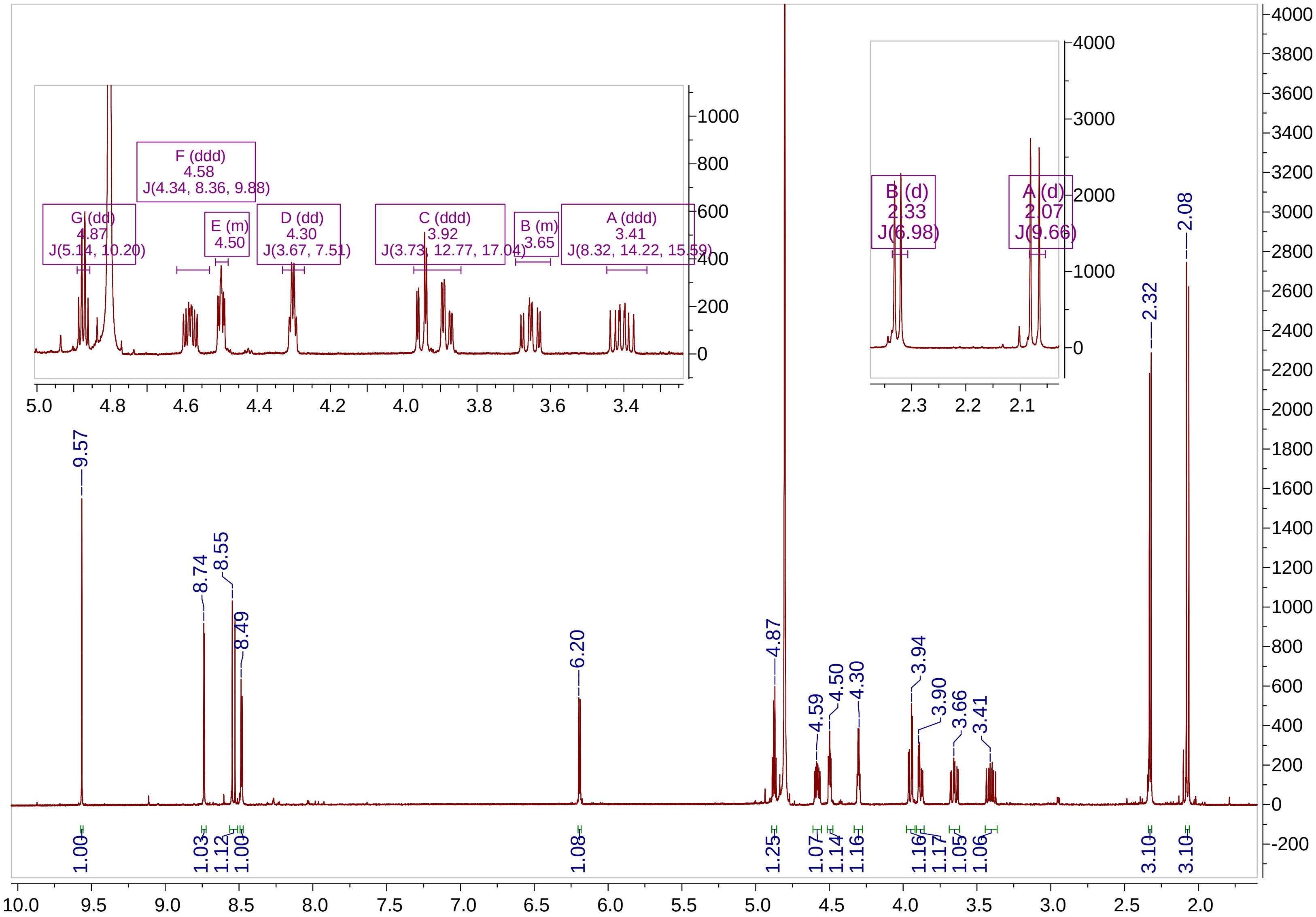

Fig. S54. **[1]H NMR spectrum of M_1MGx-A-NAC (D_2O)**

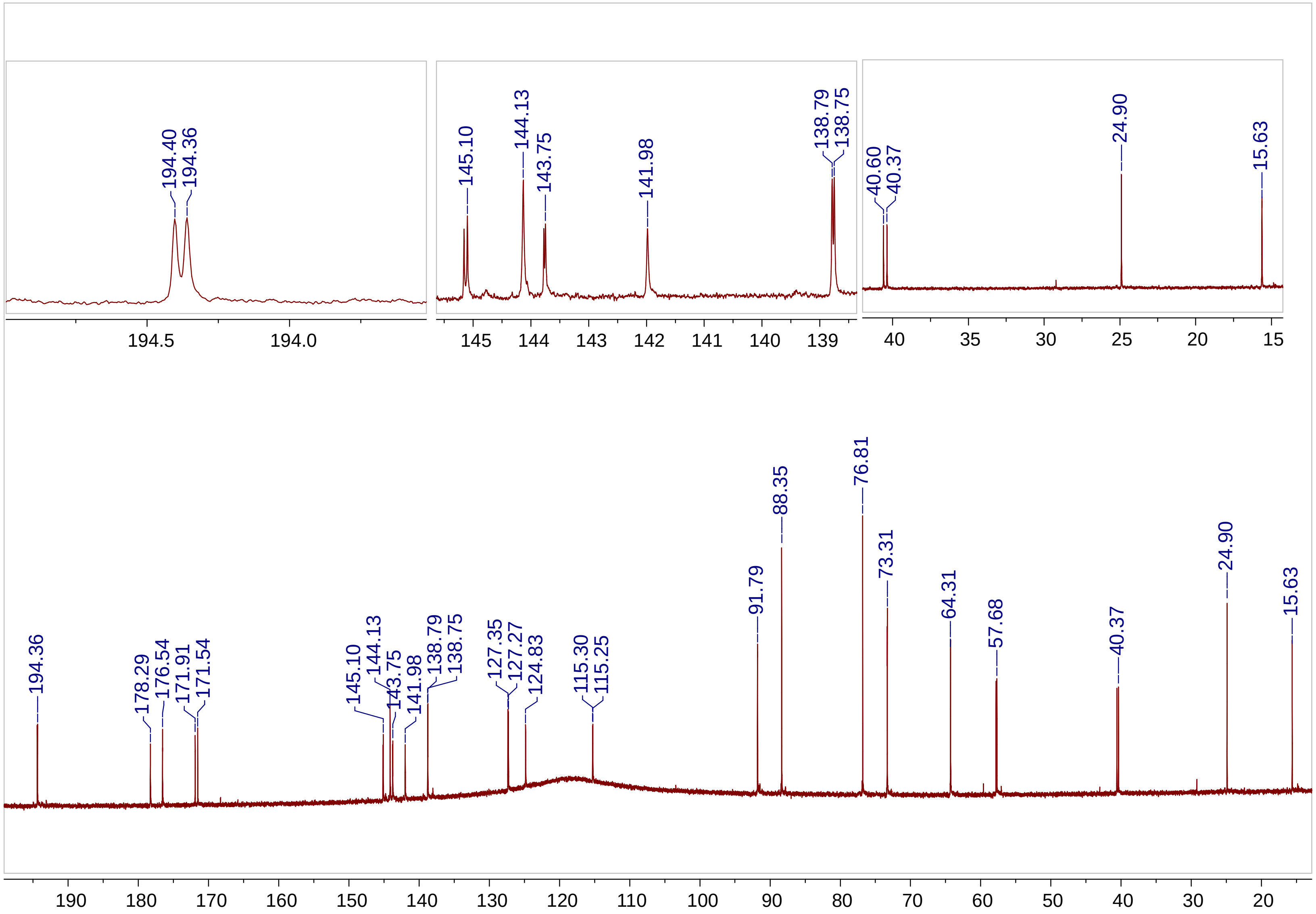

Fig. S55. ^{13}C **NMR spectrum of** M_1**MGx-A-NAC (**D_2O**)**

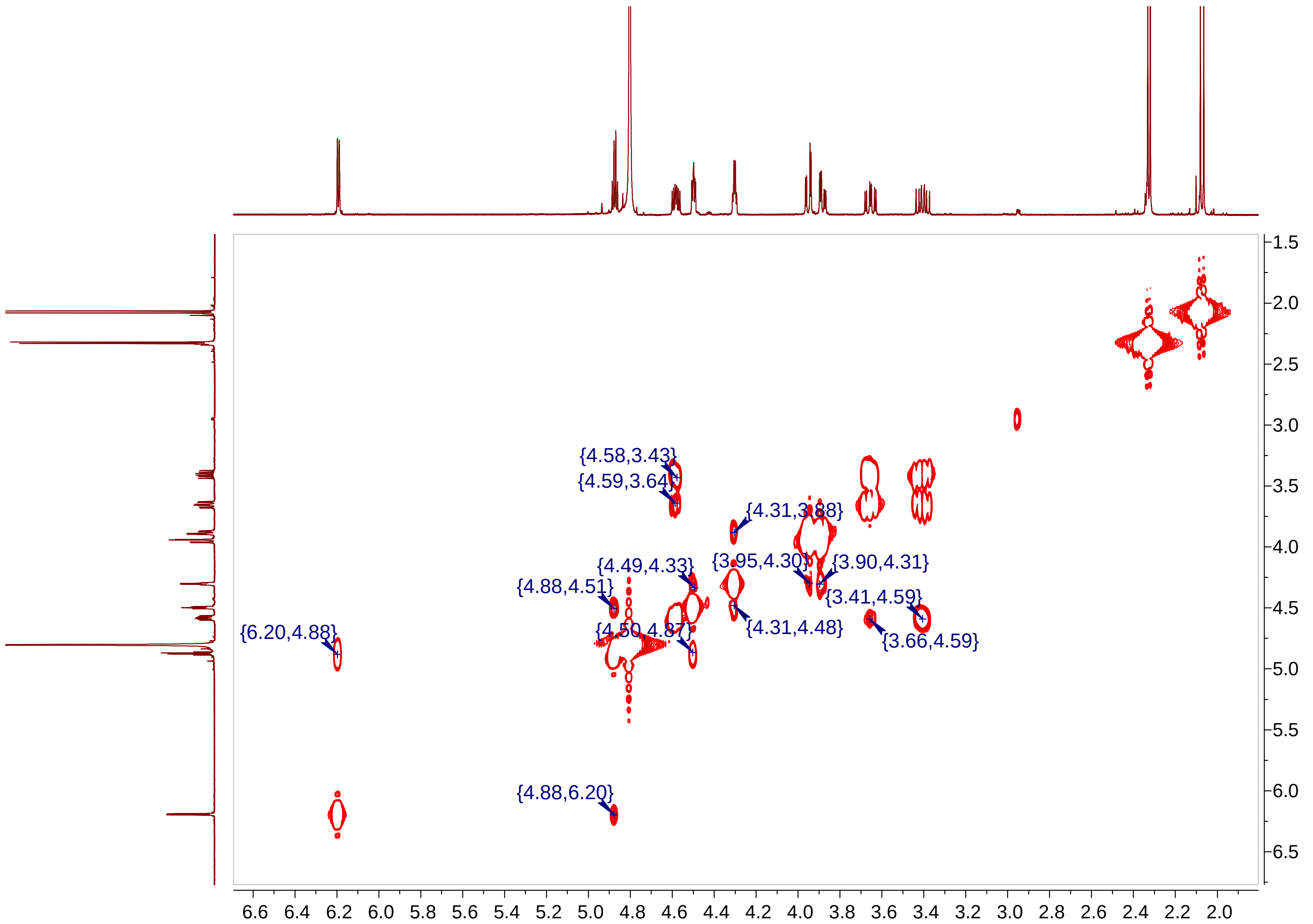

Fig. S56. COSY spectrum of M_1MGx-A-NAC (D_2O)

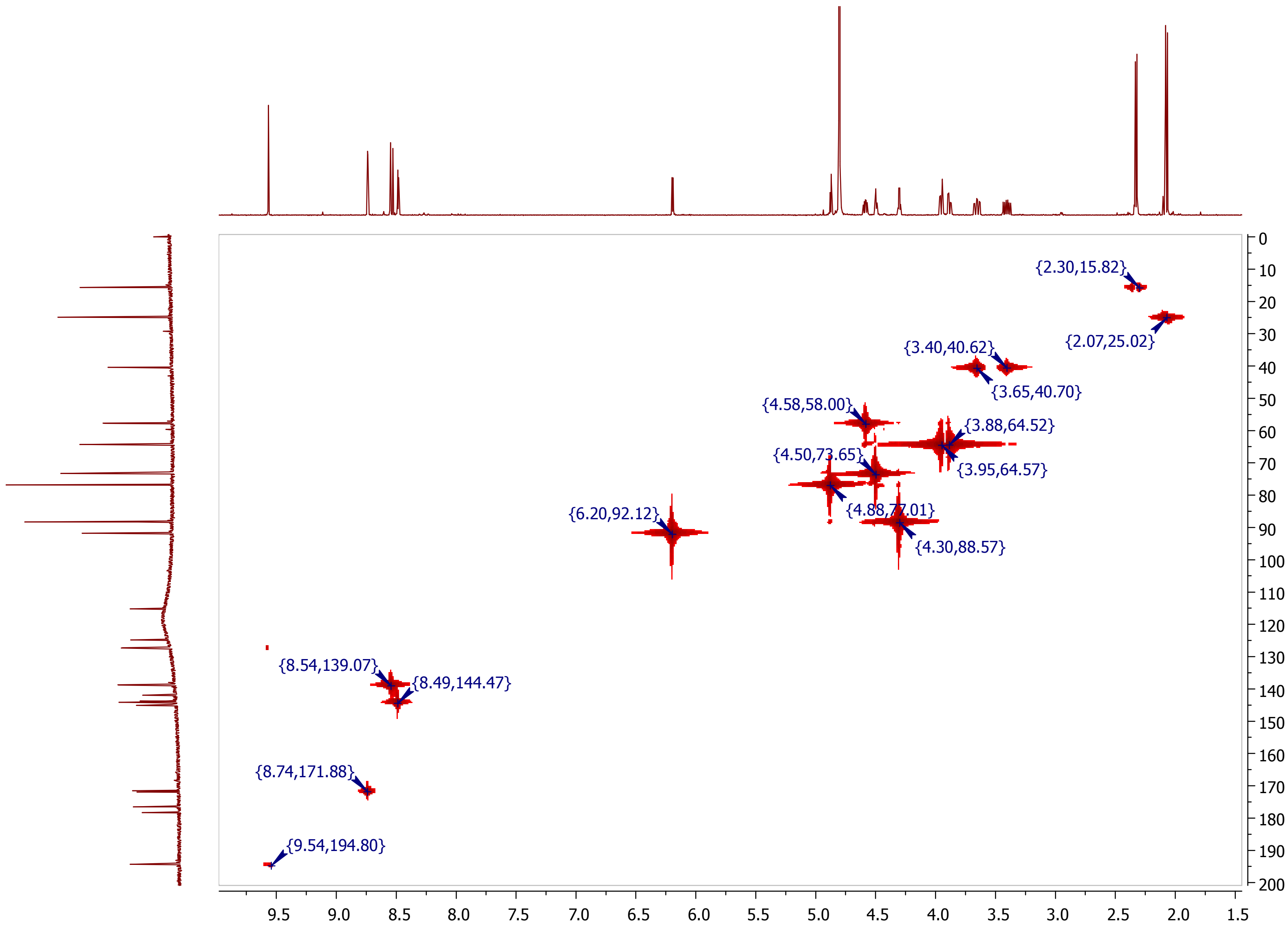

Fig. S57. HSQC spectrum of M_1MGx-A-NAC (D_2O)

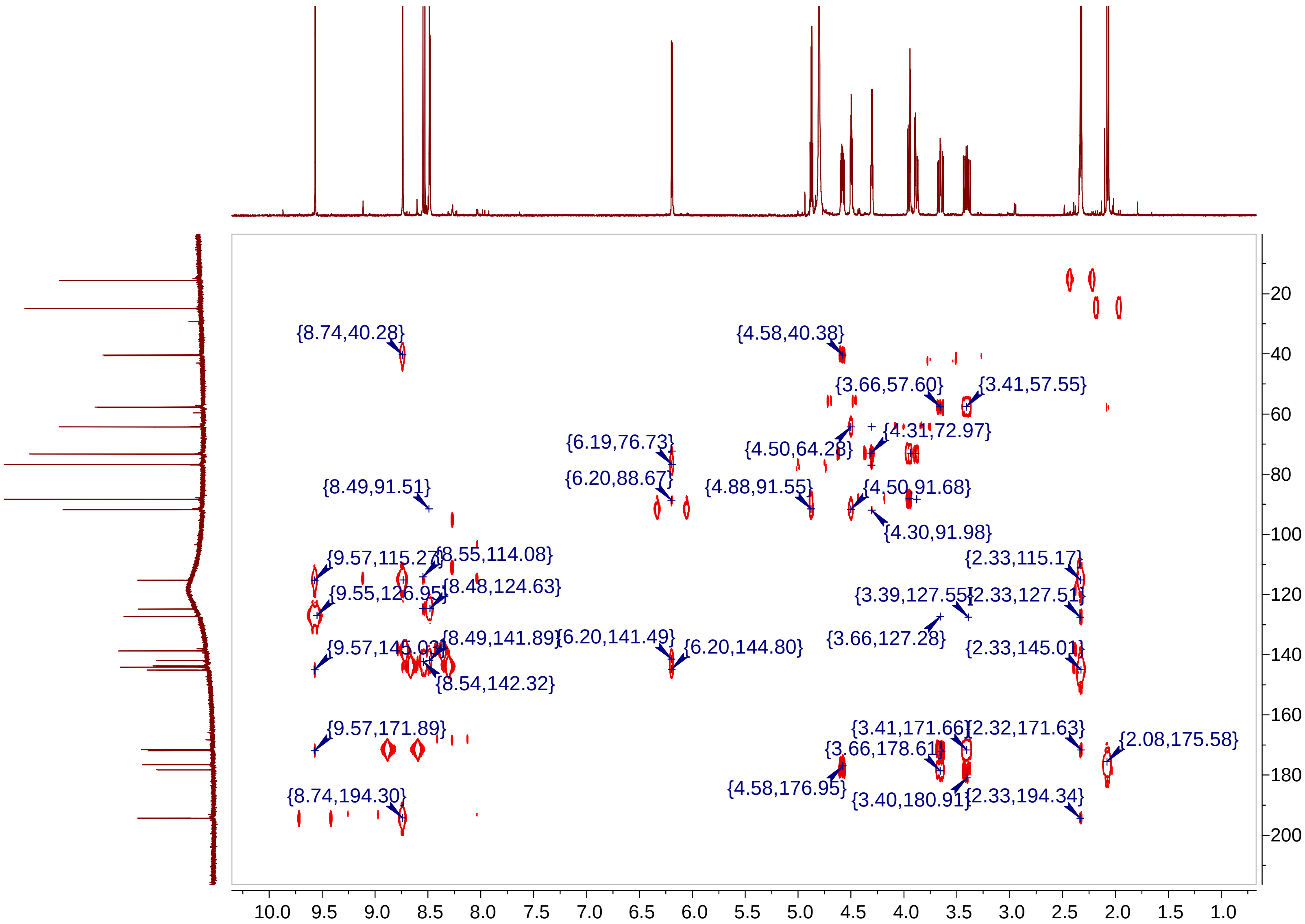

Fig. S58. HMBC spectrum of M_1MGx-A-NAC (D_2O)

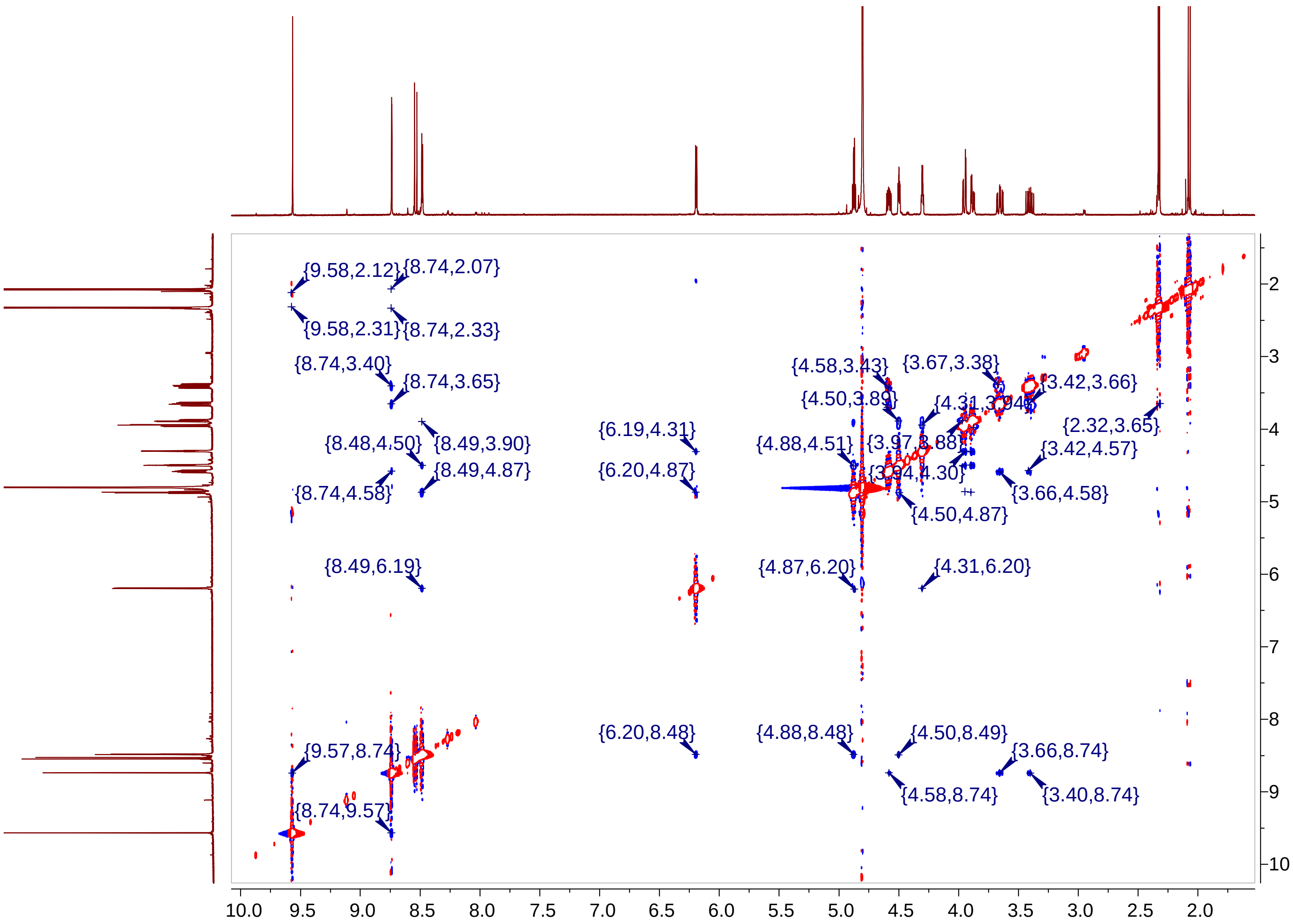

Fig. S59. NOESY spectrum of M_1MGx-A-NAC (D_2O)